The DESPEC setup for GSI and FAIR

Mistry, A. K.; Albers, H. M.; Arıcı, T.; Banerjee, A.; Benzoni, G.; Cederwall, B.; Gerl, J.; Górska, M.; Hall, O.; Hubbard, N.

Published in:
Nuclear Instruments and Methods in Physics Research, Section A: Accelerators, Spectrometers, Detectors and Associated Equipment

DOI:
10.1016/j.nima.2022.166662

Publication date:
2022

Nuclear Inst. and Methods in Physics Research, A 1033 (2022) 166662

Contents lists available at ScienceDirect

Nuclear Inst. and Methods in Physics Research, A

journal homepage: www.elsevier.com/locate/nima

The DESPEC setup for GSI and FAIR

A.K. Mistry [1,2,*], H.M. Albers [2], T. Arıcı [3], A. Banerjee [2], G. Benzoni [4], B. Cederwall [5], J. Gerl [2], M. Górska [2], O. Hall [6], N. Hubbard [1,2], I. Kojouharov [2], J. Jolie [7], T. Martinez [8], Zs. Podolyák [9], P.H. Regan [9,10], J.L. Tain [11], A. Tarifeno-Saldivia [12], H. Schaffner [2], V. Werner [1], G. Ağgez [3], J. Agramunt [11], U. Ahmed [1], O. Aktas [5], V. Alcayne [8], A. Algora [11,13], S. Alhomaidhi [1,2], F. Amjad [2], C. Appleton [6], M. Armstrong [7], M. Balogh [14], K. Banerjee [15], P. Bednarczyk [16], J. Benito [17], C. Bhattacharya [15], P. Black [6], A. Blazhev [7], S. Bottoni [4,18], P. Boutachkov [2], A. Bracco [18,4], A.M. Bruce [19], M. Brunet [9], C.G. Bruno [6], I. Burrows [20], F. Calvino [12], R.L. Canavan [9,10], D. Cano-Ott [8], M.M.R. Chishti [9], P. Coleman-Smith [20], M.L. Cortés [1], G. Cortes [12], F. Crespi [18,4], B. Das [5], T. Davinson [6], A. De Blas [12], T. Dickel [2], M. Doncel [21], A. Ertoprak [5,3], A. Esmaylzadeh [7], B. Fornal [16], L.M. Fraile [17], F. Galtarossa [14], A. Gottardo [14], V. Guadilla [11,22], J. Ha [23,24], E. Haettner [2], G. Häfner [25,7], H. Heggen [2], P. Herrmann [1], C. Hornung [2], S. Jazrawi [9,10], P.R. John [1], A. Jokinen [26], C.E. Jones [19], D. Kahl [6,27], V. Karayonchev [7], E. Kazantseva [2], R. Kern [1], L. Knafla [7], R. Knöbel [2], P. Koseoglou [1], G. Kosir [28], D. Kostyleva [2], N. Kurz [2], N. Kuzminchuk [2], M. Labiche [20], J. Lawson [20], I. Lazarus [20], S.M. Lenzi [23], S. Leoni [4,18], M. Llanos-Expósito [17], R. Lozeva [25], A. Maj [16], J.K. Meena [15], E. Mendoza [8], R. Menegazzo [24], D. Mengoni [14], T.J. Mertzimekis [29], M. Mikolajczuk [22,2], B. Million [4], N. Mont-Geli [12], A.I. Morales [11], P. Morral [20], I. Mukha [2], J.R. Murias [17], E. Nacher [11], P. Napiralla [1], D.R. Napoli [14], B.S. Nara-Singh [30], D. O'Donnell [30], S.E.A. Orrigo [11], R.D. Page [31], R. Palit [32], M. Pallas [12], J. Pellumaj [14], S. Pelonis [29], H. Pentilla [26], A. Pérez de Rada [8], R.M. Pérez-Vidal [14], C.M. Petrache [25], N. Pietralla [1], S. Pietri [2], S. Pigliapoco [24], J. Plaza [8], M. Polettini [4,18], C. Porzio [4,18], V.F.E. Pucknell [20], F. Recchia [23], P. Reiter [7], K. Rezynkina [24], S. Rinta-Antila [26], E. Rocco [2], H.A. Rösch [2,1], P. Roy [15,2], B. Rubio [11], M. Rudigier [1], P. Ruotsalainen [26], S. Saha [33], E. Şahin [1,2], Ch. Scheidenberger [2], D.A. Seddon [31], L. Sexton [6], A. Sharma [34], M. Si [25], J. Simpson [20], A. Smith [35], R. Smith [20], P.A. Söderström [27], A. Sood [5], A. Soylu [36], Y.K. Tanaka [37], J.J. Valiente-Dobón [14], P. Vasileiou [29], J. Vasiljevic [5], J. Vesic [28], D. Villamarin [8], H. Weick [2], M. Wiebusch [2], J. Wiederhold [1], O. Wieland [4], H.J. Wollersheim [2], P.J. Woods [6], A. Yaneva [7], I. Zanon [14], G. Zhang [23,24], J. Zhao [2,38], R. Zidarova [1], G. Zimba [26], A. Zyriliou [29]

[1] *Institut für Kernphysik, Technische Universität Darmstadt, D-64289 Darmstadt, Germany*
[2] *GSI Helmholtzzentrum für Schwerionenforschung, 64291 Darmstadt, Germany*
[3] *Physics Department, Faculty of Science, Istanbul University 34459 Vezneciler, Istanbul, Turkey*
[4] *INFN Sezione di Milano, I-20133 Milano, Italy*
[5] *Department of Physics, KTH Royal Institute of Technology, SE-10691 Stockholm, Sweden*
[6] *School of Physics and Astronomy, University of Edinburgh, Edinburgh, EH9 3FD, UK*
[7] *IKP, University of Cologne, D-50937 Cologne, Germany*
[8] *Centro de Investigaciones Energéticas Medioambientales y Tecnológicas (CIEMAT), Madrid 28040, Spain*
[9] *Department of Physics, University of Surrey, Guildford, GU2 7XH, UK*
[10] *Medical Marine and Nuclear Department, National Physical Laboratory, Teddington, Middlesex, TW11 0LW, UK*
[11] *Instituto de Fisica Corpuscular, CSIC-Universidad de Valencia, E-46071, Valencia, Spain*
[12] *Institute of Energy Technologies (INTE), Technical University of Catalonia (UPC), Barcelona, Spain*
[13] *Institute of Nuclear Research, Debrecen H-4026, Hungary*
[14] *INFN Laboratori Nazionali di Legnaro, Legnaro, Italy*

* Corresponding author at: Institut für Kernphysik, Technische Universität Darmstadt, D-64289 Darmstadt, Germany.
E-mail address: A.K.Mistry@gsi.de (A.K. Mistry).

https://doi.org/10.1016/j.nima.2022.166662
Received 10 December 2021; Received in revised form 3 March 2022; Accepted 23 March 2022
Available online 6 April 2022

[15] Variable Energy Cyclotron Centre, 1/AF, Bidhan Nagar, Kolkata 700064, India
[16] Institute of Nuclear Physics, PAN, 31-342, Kraków, Poland
[17] Grupo de Física Nuclear and IPARCOS, Universidad Complutense de Madrid, CEI Moncloa - E-28040 Madrid, Spain
[18] Dipartimento di Fisica, Università degli Studi di Milano, Milano, Italy
[19] School of Computing, Engineering and Mathematics, University of Brighton, Lewes Road, Brighton BN2 4GJ, United Kingdom
[20] Science and Technology Facilities Council, Daresbury Laboratory, Daresbury, WA4 4AD, UK
[21] Department of Physics, Stockholm University, SE-10691 Stockholm, Sweden
[22] Faculty of Physics, University of Warsaw, 02–093 Warsaw, Poland
[23] Dipartimento di Fisica e Astronomia, Universitàt di Padova, Padova, Italy
[24] INFN Sezione di Padova, Padova, Italy
[25] University Paris-Saclay, IJCLab, CNRS/IN2P3, F-91405 Orsay, France
[26] University of Jyväskylä, Seminaarinkatu 15, 40014 Jyväskylän yliopisto, Finland
[27] Extreme Light Infrastructure-Nuclear Physics, Horia Hulubei National Institute for Physics and Nuclear Engineering, Bucharest-Măgurele, Romania
[28] Jozef Stefan Institute, Jamova cesta 39, 1000 Ljubljana, Slovenia
[29] National & Kapodistrian University of Athens, Zografou Campus, Athens, GR-15784, Greece
[30] SUPA, School of Computing, Engineering and Physical Sciences, University of the West of Scotland, Paisley, UK
[31] Department of Physics, University of Liverpool, Liverpool, L69 7ZE, UK
[32] Tata Institute of Fundamental Research, Mumbai 400005, India
[33] Department of Physics and Applied Physics, University of Massachusetts Lowell, Lowell, MA 01854, USA
[34] Department of Physics, Indian Institute of Technology Ropar, Rupnagar, India
[35] School of Physics and Astronomy, University of Manchester, Oxford Road, Manchester, M13 9PL, UK
[36] Van Swinderen Institute for Particle Physics and Gravity, University of Groningen, Groningen, The Netherlands
[37] High Energy Nuclear Physics Laboratory, RIKEN, Wako, 351-0198 Saitama, Japan
[38] School of Physics, Peking University, Beijing 100871, China

ARTICLE INFO

Keywords:
α, β γ spectroscopy
Digital electronics
Fast timing
FAIR
DESPEC
NuSTAR

ABSTRACT

The **DE**cay **SPEC**troscopy (DESPEC) setup for nuclear structure investigations was developed and commissioned at GSI, Germany in preparation for a full campaign of experiments at the FRS and Super-FRS. In this paper, we report on the first employment of the setup in the hybrid configuration with the AIDA implanter coupled to the FATIMA $LaBr_3$(Ce) fast-timing array, and high-purity germanium detectors. Initial results are shown from the first experiments carried out with the setup. An overview of the setup and function is discussed, including technical advancements along the path.

1. Introduction

Investigation of exotic nuclei far away from the valley of stable isotopes is one of the key topics in the study of the atomic nucleus during recent decades. The production, detection, and measurement of short lived and rare nuclei is an experimental challenge that can be addressed with novel detection systems. A useful technique to obtain a first insight for these investigations is decay spectroscopy of stopped ions. The measurement of excited states in the stopped ion (in the case of longer-lived $\sim$ μs isomeric states) can be studied by observing the γ-ray emission during the de-excitation to the ground state. In addition, if the stopped ion undergoes nuclear decay, excited states both prompt and delayed temporally can be measured in the daughter nucleus following charged and neutral particle decay. These methods are extremely sensitive (down to few ions/day), as the measurement is essentially background free. Examples of such measurements can be found in [1,2].

The DEcay SPECtroscopy (DESPEC) setup is designed with the goal of measuring exotic nuclei produced via fragmentation reactions separated and identified through the FRagment Separator (FRS) [3] located at the Gesellschaft für Schwerionenforschung (GSI), and in future the Super-conducting FRagment Separator (Super-FRS) [4] based at the upcoming Facility for Antiproton and Ion Research (FAIR) [5]. A discussion and timeline of the development path of DESPEC can be found in Refs. [6–8]. DESPEC addresses a number of areas of interest in nuclear structure physics, such as decay studies of near drip-line nuclei with extreme neutron-to-proton ratios, in particular towards the neutron-rich *r*-process line.

To achieve the primary physics goals laid out, DESPEC takes advantage of the existence of nano-to-millisecond isomeric states to enable spectroscopic information to be obtained. Due to this sensitivity, DESPEC will also be able to access species produced at very low yields (0.01-100/s).

Isomeric decays and measurements of decays following β and/or proton emission can provide the γ-ray 'fingerprints' which give the first glimpses on the internal structure of nuclei. A systematic study of key experimental signatures, such as the energy of the first excited state, the ratio of the excitation energies or the decay probabilities of the lowest-lying levels in even–even nuclei, can demonstrate effects such as the erosion of the established magic numbers, and reveal the development and evolution of nuclear collective excitations (see e.g. [9]).

A key component of the DESPEC setup is the Advanced Implantation Detector Array (AIDA) which can register the implantation of ions, and correlate them spatially and temporally with their subsequent charged particle decays ($\beta^{\pm}$, α, proton, and internal conversion electrons) and thus acts as an active stopper. AIDA is surrounded by an arrangement of γ ray and neutron detectors. Ultimately the setup is flexible in terms of detector type and arrangement, with a number of configurations available from an extensive suite of detector subsystems. Such flexibility offers the advantage of selecting a given configuration to suit the physics case. The setup comprises:

- The Advanced Implantation Detector Array (AIDA) [10–12] highly-pixelated Double-Sided Silicon Strip Detector (DSSD) stopper stack.
- An arrangement of high-purity germanium (HPGe) such as the DESPEC Germanium Array Spectrometer (DEGAS) [13,14] surrounding the AIDA stack for high-resolution γ-ray detection.
- The FAst TIMing Array (FATIMA) composed of a $LaBr_3$(Ce) array [15] for γ-ray fast-timing measurements.
- The βPlastic fast-timing plastic scintillators installed up and downstream of the AIDA DSSD stack for β-decay and excited nuclear state lifetime measurements (in combination with FATIMA).
- An arrangement of neutron detectors with the BEta-deLayEd Neutron detector (BELEN) [16] or the MOdular Neutron time-of-flight SpectromeTER (MONSTER) [17] to study the β-delayed neutron-emission branch in detail.

- A γ-ray calorimeter as the Decay Total Absorption γ-Ray Spectrometer (DTAS) [18,19] for a full reconstruction of the B(GT) β-decay strength function and the possible measurement of isomeric states with high efficiency.

To accommodate the DESPEC detectors, a combined data acquisition (DAQ) system is required for merging the variety of separate, independently running detector systems.

In order to have a complete picture of the β-decay process, both high-resolution and high-efficiency studies need to be performed. The first goals are achieved by exploiting the combination of AIDA and HPGe detectors, coupled to ancillaries such as FATIMA to enhance the sensitivity to specific observables (the lifetimes of nuclear levels or delayed neutron spectroscopy). The second approach is based on total absorption spectroscopy. This can include measurement of the neutron spectrum by MONSTER, or the use of highly efficient scintillator detectors like DTAS aiming at measuring the full decay cascade rather than individual γ-rays.

From day one of the FAIR research program, DESPEC will be employed in the low-energy branch of the new facility: namely in the focal plane of the Super-FRS where the spectroscopic ability of the setup can be fully realised with higher intensity beams, purity of the ion species, and improved transmission, giving access to new regions of exotic nuclei for measurement. While waiting for the Super-FRS to come online, the DESPEC setup is employed at the GSI facility in the fourth focal plane (S4) of the FRS as part of the GSI-FAIR Phase-0 experiments. Here, the DESPEC collaboration is commissioning and investigating the capabilities of the setup in advance, and continuing the current drive in understanding the underlying structure of exotic nuclei through a series of experimental campaigns (see e.g. Ref. [20]).

The initial focus of the experimental campaign between 2019–2021 was the discovery of structural properties of $N = Z$ nuclei, heavy neutron-rich nuclei in the region around and above ^{208}Pb; and nuclei in the proximity of ^{100}Sn.

The purpose of this article is to provide a description of each detection element to be employed with DESPEC, and to present first experimental results that illustrate the performance and use with the first iteration of the setup.

2. Overview of the setup

In this section, a description of the single subsystems used in the campaign 2019–2021 for high-resolution studies is presented, plus additional subsystems the are planned to be used in future DESPEC campaigns and have so far been deployed at other facilities.

The DESPEC setup is located in the S4 focal plane of the FRS [3], which serves the purpose of the production and in-flight separation of secondary fragment (or fission) ions of interest. The FRS is coupled to the SIS18 synchrotron, where the stable beam species accelerated up to 1 GeV/nucleon are impinged upon thick targets ranging from 1 to 8 g/cm^2 Be and Pb material to produce fragment ion species. The typical beam energies received from the SIS18 range from 4.5 GeV/u for hydrogen, up to 1 GeV/u for uranium. After the target, a combination of magnetic elements (dipoles, quadrupoles, and sextupoles), degrader elements and slits ensure the selection and transport of the fragments. Ion species up to a magnetic rigidity of Bρ = 18 Tm can be separated using the Bρ − ΔE-Bρ method [3]. A schematic of the FRS setup can be found in [21]. (Note: in the given reference the focal plane areas are referred to as F1–F4, in our work we refer to the corresponding experimental areas S1–S4). The separator can be used in monochromatic and achromatic modes depending upon the experimental requirements. A wedge-shaped degrader at S2 is used to achieve either the achromatic or monochromatic modes. Typically, the separator is operated in achromatic mode, where the final fragment position is independent of the initial momentum and angular spread, such that ions with the same Bρ can be focused to the same point at the focal plane.

Optimal reduction of contaminants arriving to the S2 dispersive focal plane is achieved by using X-directional slits in focal plane S1. Passive elements through the separator can help to reduce contaminants and select the species of interest. These include X-directional slits, located at the S1, S2, S3 and S4 focal planes, while an additional homogeneous degrader in S1 position is used in specific cases. For better separation, and to minimise the production of charge states while interacting with material in the separator, the energy of the fragments is typically kept as high as possible, above 400 MeV/u at the entrance of the FRS detectors in the S4 area. Therefore, the use of an S4 degrader is required to reduce the ion energy enough to ensure implantation of the ions into the AIDA stack of Si detectors.

Particle identification is achieved using the Bρ-TOF-ΔE method, for which both the exact reconstruction of the position at S2 and S4 and the Time-Of-Flight (TOF) between the two focal planes have to be measured with precision. In the S2 and S4 focal plane areas, a pair of TPC (Time Projection Chamber) position detectors, are employed for precise position determination, matching the requirement of 1 mm (FWHM) position resolution, crucial for a correct reconstruction of the trajectories. Fast plastic scintillator detectors in the two focal planes ensure the measurement of the TOF.

High rates at the S2 focal plane might limit the performance of the scintillator detectors. Therefore a segmented plastic detector known as Finger composed of several plastic scintillator elements, each one read individually and capable of high rate mode, is currently under development. In addition this detector will give enhanced position resolution, comparable or better than the TPC detectors.

The charge of the ions is measured with the help of two Multiple Sampling Ionization Chamber (MUSIC) detectors with a stripper foil in between. An additional scintillator, located after the S4 degrader, helps with the identification of unreacted ions reaching the AIDA stopper.

Fig. 1 shows a photograph of the hybrid setup used in 2021 using the EUROBALL 7-fold clusters [22] coupled to the FATIMA $LaBr_3$(Ce) array. In Fig. 2, 3D renderings of the mechanical setup are shown. The DESPEC setup exploited in the 2019–2021 experimental campaigns consisted mainly of the AIDA stack of Si detectors, sandwiched between two plastic (βPlastic) detectors and surrounded by a composite array of γ-ray detectors. In the following, a description of the components, including read-out and performance, is given.

2.1. AIDA

The AIDA detector array is based on Double Sided Silicon-strip Detectors (DSSD) characterised by a high degree of pixelation. The energetic (100–200 MeV/u) exotic heavy-ions, selected and transported by the FRS are slowed by a series of degraders and implanted into a stack of DSSDs with a variable number of layers, to ensure a correct implantation depth for several species at the same time. AIDA has been exploited in several other campaigns such as at RIKEN. A detailed description and utilisation of AIDA in these campaigns can be found in [10–12,23]. The implanted nuclei undergo radioactive decay emitting low-energy β and α particles, protons, neutrons and γ rays. The charged particles are detected by the DSSDs. Each unit is based on 8 × 8 cm^2 DSSDs with thickness of 1 mm, composed of 128 × 128 strips (16384 pixels), with a 0.560 mm inter-strip pitch. The DSSDs are purchased as single (8 × 8 cm^2) wafer or triple (24 × 8 cm^2) wafer devices. Therefore, AIDA can be employed either as a 'single' stack with the narrower 8 × 8 cm^2 wafers, or in a 'triple' stack configuration with the wider 24 × 8 cm^2 DSSDs, selected depending upon the expected ion-implant distribution. Photographs of the single (top left) and triple (top right) configurations mounted in the stack are shown in Fig. 3. During the experimental runs, the stack of DSSDs are enclosed within an external aluminium casing, known as the AIDA 'snout'. The dense pixelation allows for the position in X, Y, Z (depth) where the nucleus has been implanted to be correlated to the subsequent decay particles. The measurement of the time elapsed between the implantation and the subsequent decay returns the half-life of the radioactive decay.

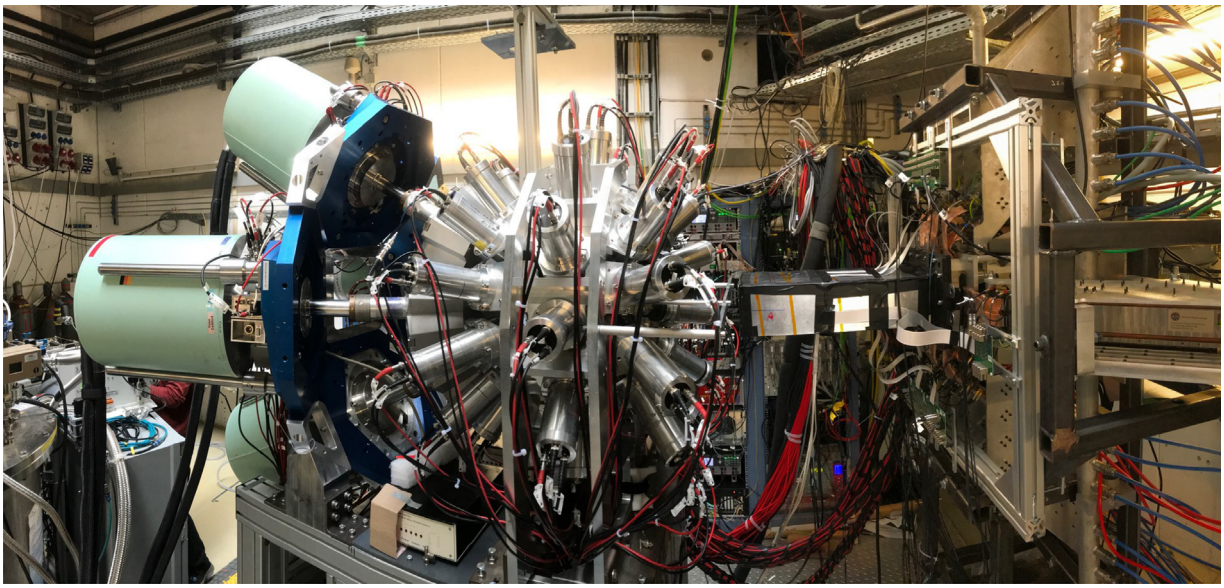

Fig. 1. Experimental setup used in the campaign in 2021, where the coupling of the EUROBALL detectors (with green dewars) and the FATIMA crystals (in the grey aluminium cases) are clearly visible. The γ-ray detectors are retracted from the AIDA snout (enclosure containing the DSSDs) which is visible on the right.

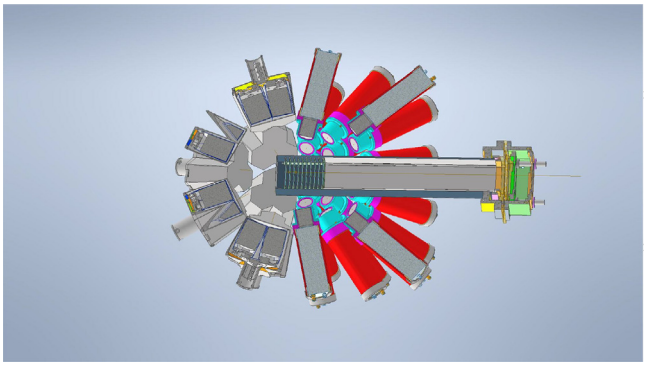

Fig. 2. 3D rendering of the DESPEC hybrid setup including FATIMA and HPGe detectors surrounding the AIDA snout.

The energy deposited by the implant in the DSSD is of the order of several GeV, while the energy of the subsequent decay events is of the order of ~50 keV to a few MeV. The average time between implantation and decay ranges between tens of ms to several tens of seconds. In order to cope with the large number of channels and the need to measure energies over a multi-order of magnitude dynamic range, an Application Specific Integrated Circuit (ASIC) chip was developed [24]. The system is able to measure charged particle energies over two (high and low) energy ranges, autonomously switching between them. It also has a fast recovery time of <40 μs. The operation of the ASIC (including the slow-comparator-controlled analogue multiplex and ADC readout) is synchronised by a 500 kHz clock. ADC data is timestamped using an internal 100 MHz clock and ADC data timestamps therefore increment at 2 μs intervals — sufficient for ion implantation-decay-gamma correlations. Fast comparator data are also available and timestamped using the internal 100 MHz clock — the fast comparator timestamps therefore increment at 10 ns intervals. The higher bandwidth required for a fast comparator necessarily means a lower signal:noise ratio and therefore a higher energy threshold compared to the slow comparator.

The AIDA hardware consists of a number of 64-channel FEE64 modules that control and process the data from 4 × 16-channel AIDA ASICs. Each FEE64 operates as an independent DAQ and can handle data rates of up to 500k data-items/s. Each FEE64 also accepts a single external NIM signal which is recorded and timestamped at 10 ns resolution, allowing simple correlation data to be recorded. Four FEE64 modules are necessary to read out one single-wafer DSSD, while eight are necessary for one triple-wafer DSSD. The current infrastructure is capable of supporting 16 FEE64 modules (4 single wafers, or 2 triple wafers) with up to 24 FEE64s possible in the near future (3 triple wafers).

Typically, the low-energy slow comparator threshold for β-decays is around 100 keV. The measured β efficiency of ≈35% is strongly related to the software energy threshold, the implantation profile, the β-decay end point energy, and the heavy-ion implant/veto conditions applied. β-decay events are identified as clusters of adjacent active pixels. The majority (>85%) of decay-event clusters consist of a single pixel, while most of the remainder are made of two pixels. For implant-event clusters, it is more common for two strips on each side to fire.

AIDA runs as a triggerless system [25], and the FEE64 DAQ produces time-ordered data items with a 64-bit White Rabbit timestamp [26] using the Total Data Readout (TDR) GREAT format [27]. The White Rabbit timestamp and 200 MHz clock are provided via HDMI cables from dedicated White Rabbit receiver modules (VETAR2, PEXARIA5) and distributed to all AIDA FEE64s via MACB clock distribution modules. All necessary clocks within the FEE64 are derived from, and synchronised to, the input 200 MHz clock from the White Rabbit modules. This synchronises the system both to other AIDA FEE64 modules as well as the other DESPEC subsystems. The independent FEE64 DAQs run the MIDAS Data Analysis package [28]. MIDAS forwards data over a dedicated gigabit ethernet network to a high-performance workstation, which then merges the data streams from all the FEE64 DAQs, producing a single time-ordered data stream. This final datastream is subsequently saved to local disk and forwarded over gigabit ethernet to an MBS foreign data receiver.

AIDA was employed for the 2019–2021 experiments at GSI in both wide (6 DSSDs (3 side-by-side) in a two layer stack) and single (3 DSSDs in a three layer stack) configurations. An example of the single stack AIDA employed is shown in the lower photograph in Fig. 3, coupled to the electronics.

2.2. βPlastic

βPlastic is a fast-timing plastic detector designed for measuring β particles with an energy range of ~80 keV to 8 MeV. The AIDA DSSD stack is sandwiched in between two βPlastic detectors as can be

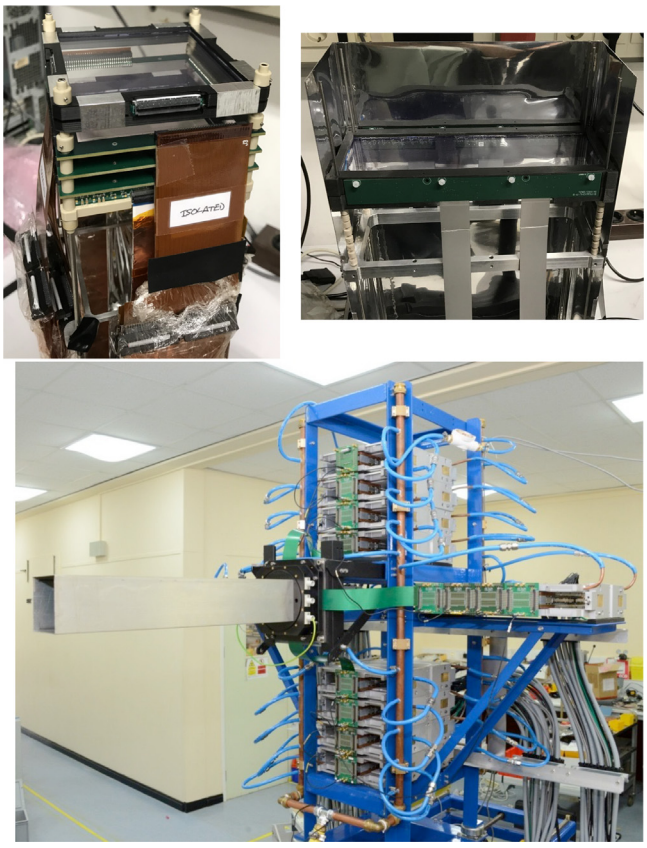

Fig. 3. Top photograph left: The arrangement of three layers of AIDA DSSD chips in the narrow configuration coupled to one of the βPlastic detectors (on top), ready to be inserted into the snout. Top photograph right: AIDA in the wide configuration. Bottom photograph: The built AIDA detector system: the snout on the left contains the several layers of the narrow 8 × 8 cm^2 DSSDs, while the blue frame hosts the electronics. The blue pipes contain the cooling medium for the electronics.

seen in the top two photographs in Fig. 3. The downstream βPlastic detector can be seen as placed above the DSSD stack. Each βPlastic detector is composed of a quadrilateral 3 mm thick sheet of scintillating plastic material (type BC-404 [29]) coupled to 3 × 3 mm^2 silicon photomultipliers (SiPMs) SensL C-Series [30] along the four sides. The excellent timing properties of such scintillating detectors allow high-precision time information for decays originating from implanted ions inside AIDA to be measured. The β particles detected with a preceding ion implantation registered in AIDA are correlated with the βPlastic detector in order to achieve fast-timing for short lived excited nuclear states, and β-decay measurements. A time resolution of ∼450 ps FWHM for 511 keV γ rays was measured using a ^{22}Na source, where the 511 keV photon emitted in the opposite direction was detected by a $LaBr_3$(Ce) detector.

The SiPMs are attached to the scintillating material via an optical coupling pad that is kept in place using a custom-fitted housing. Early iterations of the detector design included glued SiPMs, but this was found to produce too much mechanical stress on the plastic. The SiPM signals are read out by custom-made, shielded flat cables and then pass through 'booster boards', which provide an amplification factor of ∼10. The amplified signals are then accessible by Lemo outputs and fed into FPGA-based TAMEX cards with TwinPeaks front-ends, developed in-house by the Experimental Electronics Department at GSI [31]. See Section 2.3 for more details.

The detector dimensions orthogonal to the beam direction, the number of SiPMs, and the SiPM-readout schemes are flexible and can be tailored to the specific needs of the experiment. To date, configurations of 8 × 8 cm^2 (single) and 24 × 8 cm^2 (wide) have been in operation, in

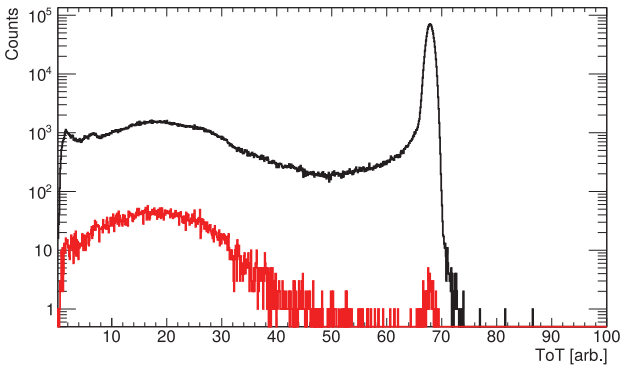

Fig. 4. Typical time-over-threshold (ToT) distributions for a single βPlastic channel. The fragment setting was for ^{34}Si. Events associated with large energy deposition and saturation of the SiPMs (predominantly due to heavy ions) are seen at channel ∼70 in black. The red distribution shows events wherein a coincident decay was measured in both AIDA and FATIMA.

conjunction with the single and wide AIDA DSSD stacks, respectively. For the single geometry, SiPMs were arranged such that each group of four was coupled to a read out, resulting in a total of 16 channels (4 along each side). In the wide geometry, SiPMs were grouped in pairs to increase the granularity, such that each long (24 cm) and short (8 cm) edge comprised 48 and 16 SiPMs coupled to 24 and 8 read-out channels, respectively, resulting in a total of 64 channels.

The time differences between leading- and trailing-edge discriminator threshold crossings (time-over-threshold, or ToT) are proportional to the amount of light collected by the SiPMs. A typical ToT distribution for a single βPlastic channel measured in-beam is shown in black in Fig. 4. The peak visible at channel ∼70 corresponds to very high energy deposition and saturation of the SiPMs due primarily to heavy-ion interactions. The broad, lower energy distribution corresponding to β particles (wherein a coincident decay event was registered in both AIDA and FATIMA) can be seen in the red spectrum.

The βPlastic detectors may also be used as implantation devices themselves, and can provide a high-efficiency veto of unwanted light ions that may pass through the AIDA DSSD stack without being stopped.

2.3. FATIMA

The FAst TIMing Array (FATIMA) [15] can be used to determine the lifetime of nuclear states down to the picosecond level, as well as measure longer-lived isomeric states. This is achieved by measuring the time difference between two detected γ rays in a decay cascade. In addition, the time difference between a γ-ray in FATIMA, and a β-particle detected by the βplastic detector can be measured; in combination with HPGe detectors the $\beta - \gamma - \gamma$ fast timing method can be applied [32].

The array used at DESPEC is a modular system of $LaBr_3$(Ce) crystals, each with 1.5" diameter and 2" length. The array has been designed in a way such that the detector number and size, as well as angular coverage, can be customised according to an experiment. In the standard DESPEC configuration, FATIMA consists of three rings with 12 detectors in each. The scintillators are coupled to fast R9779 photomultiplier (PMT) tubes. Each detector is equipped with a removable lead shield of 4 mm thickness around the crystal to minimise scattering among neighbouring detectors.

Signal processing and data acquisition are based on VME and TAMEX electronics, in mutually independent modes of operation. However, in both modes, the DAQ triggers are generated only by the FATIMA detectors. This is done to maximise the efficiency of collecting and measuring isomers.

For the VME-DAQ, the detector dynode signals are processed by V1751 CAEN digitisers. They are operated using the Digital Pulse Processing-Pulse Shape Discrimination (DPP-PSD) firmware provided

by CAEN. The digitiser offers a sampling rate of 1 GS/s, fast enough to allow several samples on the signal rise time of the FATIMA $LaBr_3$(Ce) detector. The energy information is obtained via signal integration above a dynamically determined base line level (charge to digital conversion, QDC). For time pick off of the anode signal of the detectors, CAEN V812 constant fraction discriminator (CFD) modules are used. For time measurements the CFD signals are fed into V1290 time to digital converters (TDC) modules. Each TDC board has 32 channels which take ECL input. The time resolution offered by CAEN TDC modules is 25 ps LSB (least significant bit) with a 21 bit range. The manufacturer gives an RMS time resolution of 35 ps for the individual final TDC measurement.

For the TAMEX-DAQ, an in-house developed pulse-processing technology is used [31]. The department of experimental electronics at GSI has developed TAMEX cards with TwinPeaks front-end (in addition for the βplastic detector, see Section 2.2), customised to FATIMA-PMT signal pulses. TAMEX are FPGA-based TDC modules with a time resolution of 11 ps, which are used to measure the leading edge of pulses, as well as the width of the pulses. TwinPeaks offer a very compact design (16 LEMO channels per card), while using two discrete amplifiers to process the PMT pulses. Each amplifier has a dedicated function. The high bandwidth amplifier is sensitive to small amplitude pulses generated by the PMT, and the time-over-threshold (ToT) times have a logarithmic dependence on the detector pulse charge/deposited energy. The linear amplifier offers a linear relation between deposited energy (∼ pulse charge) and pulse width (ToT). The logarithmic branch data are used to extract the timing information, by calculating the time difference between leading edges of pulses generated by consecutive γ rays. The energy information of these pulses is calculated as the ToT, which corresponds to the widths of the pulses. TAMEX offers the highly demanded features of low dead time (20 μs), high data throughput (≈85%) and long collection window (≈320 μs).

The time resolution for FATIMA obtained using the two main γ-ray transitions from a ^{60}Co source was 320 ps FWHM, with an energy resolution of 5% at 511 keV. With effective analysis techniques such as the mirror symmetric centroid difference method [33], one can extract lifetimes of states down to ∼10 ps.

2.4. High-purity germanium

For DESPEC experiments that focus on fast timing measurements of nuclear states e.g. with FATIMA, HPGe detectors are required for monitoring the spectral composition of the decaying implants. For that purpose, only moderate efficiency is needed and thus Ge-detector arrangements using the open solid angle of FATIMA downstream of AIDA can be used.

For the first DESPEC experiments, two arrays were available: up to 7 GALILEO [34,35] triple Ge Clusters (GTC) forming a calotte at forward angles, and a setup of four EUROBALL [22] seven-fold Clusters forming a cross in the forward direction. The GTC detectors closely follow the geometry of the DESPEC DEGAS detectors (see below for more details) and thus enabled detailed investigation of the response of such detectors with the environmental conditions at the FRS. Fig. 5 shows the energy dependent efficiency obtained with this setup using a ^{152}Eu source with 13 crystals, and extrapolated to 21 crystals. At 1 MeV the measured efficiency in add-back mode was 1.5%.

The experiments in 2021 employed the EUROBALL Cluster array, which provided 28 crystals, subtending a larger solid angle. With this setup the add-back efficiency at 1 MeV amounted to 3%.

Both detector setups were read out by 14 bit 100 MHz FEBEX digitisers developed at GSI [36]. An on-board FPGA is used to apply a trapezoidal filter algorithm to obtain energy information, while time information is determined from the on-board constant-fraction discriminator. Synchronisation with the other subsystems is achieved by White Rabbit timestamps. The energy resolution obtained varied between 2.3 keV and 3.1 keV at 1.3 MeV. These values are comparable

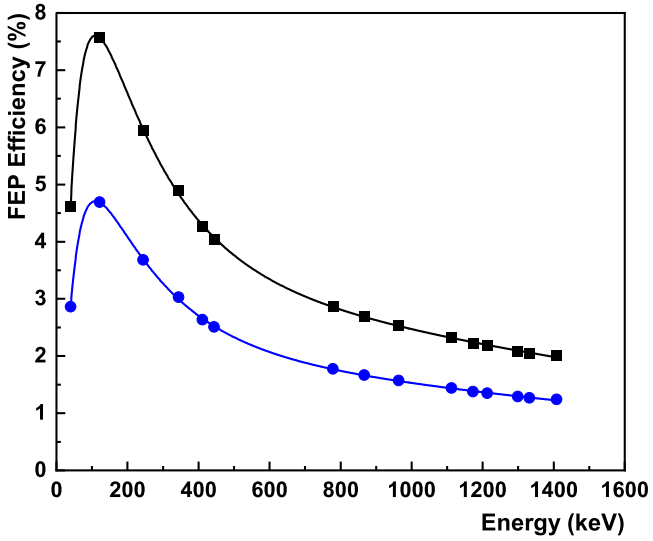

Fig. 5. Energy dependent full-energy peak (FEP) efficiency in add-back mode of the GALILEO HPGe array used in conjunction with FATIMA. Blue circles the efficiency for 13 GTC detectors using a ^{152}Eu source, black squares scaled to 21 detectors. Fits to the data points are included to guide the eye.

with the same electronics under laboratory conditions for the chosen 10 MeV energy range. The strength of the prompt radiation flash during implantation varied as expected with the charge of the implanted isotopes. It is interesting to note that besides the electromagnetic radiation, light particles were also observed. They caused oscillations in the signals of the preamplifiers lasting for up to 1 ms, and despite moderate intensities in the few Hz region, crystals protruding into the beam acceptance region of the FRS showed signs of radiation damage. Therefore, it is concluded that the light particles must have energies of several 100 MeV. Most likely they are protons and deuterons knocked out from the primary beam at the production target of the FRS. Depending upon the FRS setting, such particles may be transported to the S4 focal plane. This occurred with all beam combinations, however was most notable for the heavier beam reactions (^{208}Pb and above). In addition, the oscillations were observed in experiments where the detectors were positioned closer to zero degrees. In future this situation is likely to improve due to the double stage separation of the Super-FRS.

For the planned high-resolution γ-ray spectroscopy experiments, the DESPEC Germanium Array Spectrometer (DEGAS) will be used. DEGAS is a high-resolution, high-efficiency HPGe array for the detection of electromagnetic decays from exotic nuclear species [10]. The design exploits the EUROBALL cluster detectors, rearranged into clusters of three detectors (triple clusters).

For optimal solid angle coverage, detector units comprise three crystals in a common cryostat, electrically cooled to facilitate a compact detector geometry. Electrical cooling also provides the wanted flexibility to use DEGAS modules for other FAIR experiments in liquid nitrogen-free zones. However, in its first realisation, DEGAS will use liquid nitrogen as a cooling medium.

To further improve the sensitivity of the array as compared to RISING [37], shielding of the environmental background with active and passive components is planned. Shielding directly behind the HPGe detectors will be based on the concept of the EUROBALL 'back-catcher' veto BGO scintillation detectors. In addition, side shields from CsI(Tl) crystals will fill the gaps around the HPGe setup. Finally a lead wall will shield from background coming with the beam. DEGAS is designed to cover an implantation area of about 24 × 8 cm^2, demanded by the wider focal plane of the Super-FRS at FAIR and well suited for the focal plane of the FRS.

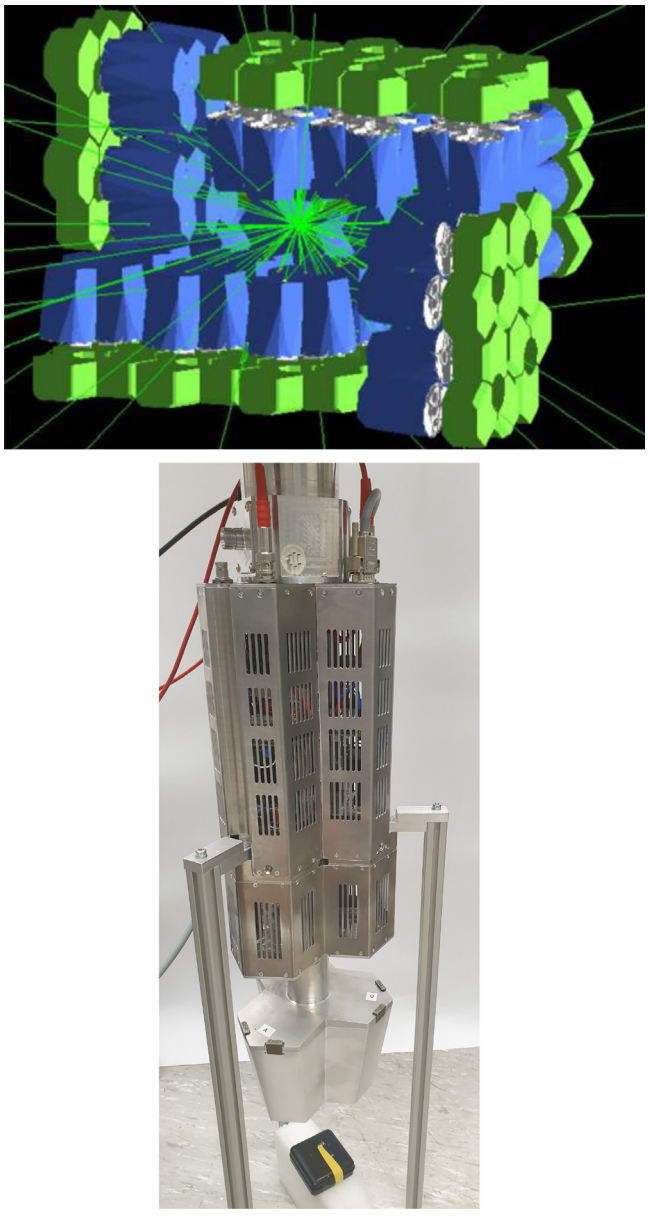

Fig. 6. Upper plot: 3D rendering of the DEGAS setup comprising 28 triple Ge crystals surrounding the active stopper. Lower photograph: Prototype of the DEGAS triple detector equipped with liquid nitrogen cooling and external HV supply.

The on-board electronics include low-noise pre-amplifiers with overload recovery (in case of high-energy particle hits), high-voltage generators, power management and temperature controls. The slow control data is read out together with the physics data stream through EPICS [38].

The compact configuration of DEGAS surrounding the AIDA detector was optimised by Monte Carlo GEANT4 simulations as shown in the upper plot of Fig. 6. The device has been simulated in different configurations (see e.g. [13,14,39]). This final arrangement consists of 28 triple crystal HPGe detectors that surround the AIDA implantation area of 24 × 8 cm^2: 8 detectors on the back, 6 on the top and bottom, and 4 on each side. In Fig. 7 shows the full energy efficiency of this setup, 49% at 200 keV and 18% at 1.3 MeV, assuming addback only within a Cluster. Based on recent measurements, dead time losses up to 20% need to be taken into account [13].

In Fig. 6 the lower photograph shows the prototype of the DEGAS triple detector. This detector revealed an energy resolution of 1.9 keV

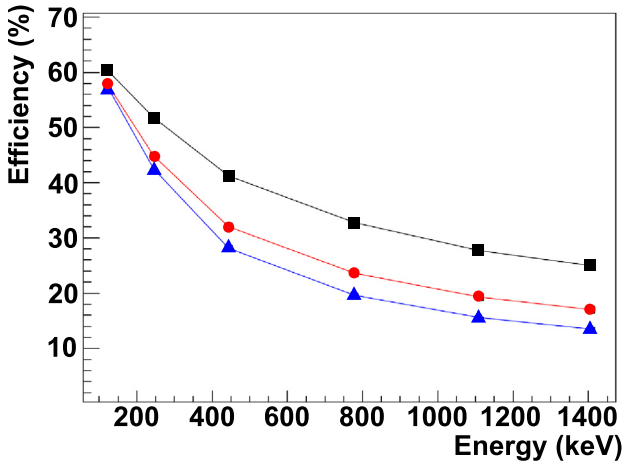

Fig. 7. Simulated peak efficiency for DEGAS as function of the γ-ray energy. The three lines correspond to Ge single crystal (blue triangle), Ge triple Cluster (red circles) and Ge calorimeter (black squares) add-back modes. The red option is the one implemented in the experiments, while the last one corresponds to summing of the energies of all responding crystals of the array.

at 1.3 MeV γ-ray energy, demonstrating the high quality of the design. After successful testing of the mechanical cooling scheme, the DEGAS detectors are being assembled and the full realisation of the setup is expected in the near future.

2.5. DTAS

The Decay Total Absorption γ-ray Spectrometer (DTAS) is a high efficiency, close to 4π γ-calorimeter with the primary aim of measuring accurately the full β-decay intensity distribution. Refs. [18,19] provide an in-depth discussion of the design and experimental characterisation of the spectrometer. After a study of possible detector materials and geometries, a flexible modular design based on the well-known NaI(Tl) scintillators was chosen. Typically sixteen modules with crystal dimensions 15 × 15 × 25 cm^3 can be arranged surrounding AIDA (see upper photograph of Fig. 8). For single γ rays, the total detection efficiency is larger than 80% for E_γ < 200 keV and the peak efficiency is larger than 60% for 200 keV < E_γ < 1 MeV and drops smoothly to 45% at 5 MeV (see lower panel of Fig. 8). The total efficiency for decay detection depends on the de-excitation path but is typically close to 100%. The energy resolution during experiments is kept at 6.9% at 1 MeV and 3.0% at 5 MeV due to a PMT gain correction system based on a pulsed light source. The modularity of DTAS provides information on energy and multiplicity distributions of decay cascades, which not only helps to constrain uncertainties in the analysis, but also provides additional relevant physical information. This expands the scope of the spectrometer, which can be viewed in this regard as a low resolution, high-efficiency γ-ray detection array (see lower panel of Fig. 8).

Background control and correction is an important issue in this type of measurement. A heavy lead shielding surrounding the setup reduces significantly the ambient background, which becomes basically negligible after β-tagging with AIDA. In the case of measurements of β-delayed neutron emitters, neutron interactions in DTAS occurring with a large probability can become an issue. However this type of background can be efficiently suppressed using timing information [41].

The full assembly was commissioned using low energy radioactive beams from the IGISOL IV facility at the Cyclotron Laboratory of the University of Jyväskylä [19,42], and took data published in [41,43–46]. A summary of the results obtained in the IGISOL IV campaign can be found in [47]. Recently the spectrometer, in combination with AIDA, was installed at the RIBF facility in RIKEN and performed a measurement of decays at and around ^{100}Sn [48].

DTAS will be used as a part of DESPEC in the 2022 experimental campaign.

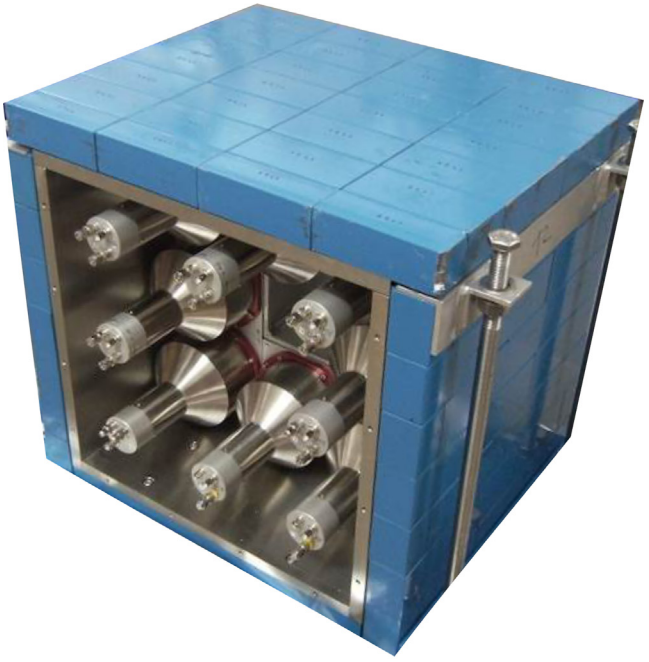

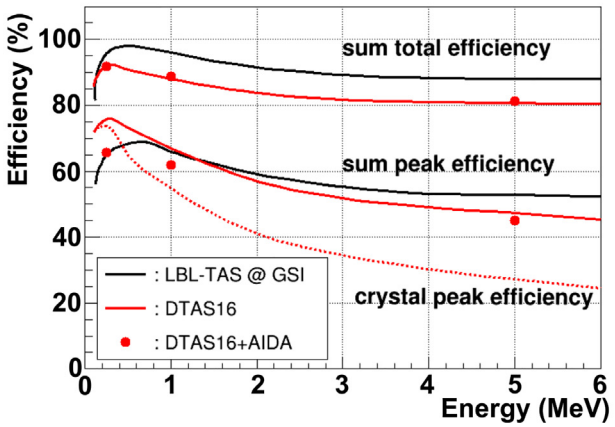

Fig. 8. Upper photograph: View of one half of DTAS set up with shielding. Lower panel: Comparison of Monte Carlo simulated total and peak efficiencies for sum signals of bare DTAS (red) and with the LBL-TAS single crystal spectrometer (black) [40]. The impact of including AIDA is shown (filled circle). Also depicted is the integrated single crystal peak efficiency (dashed line).

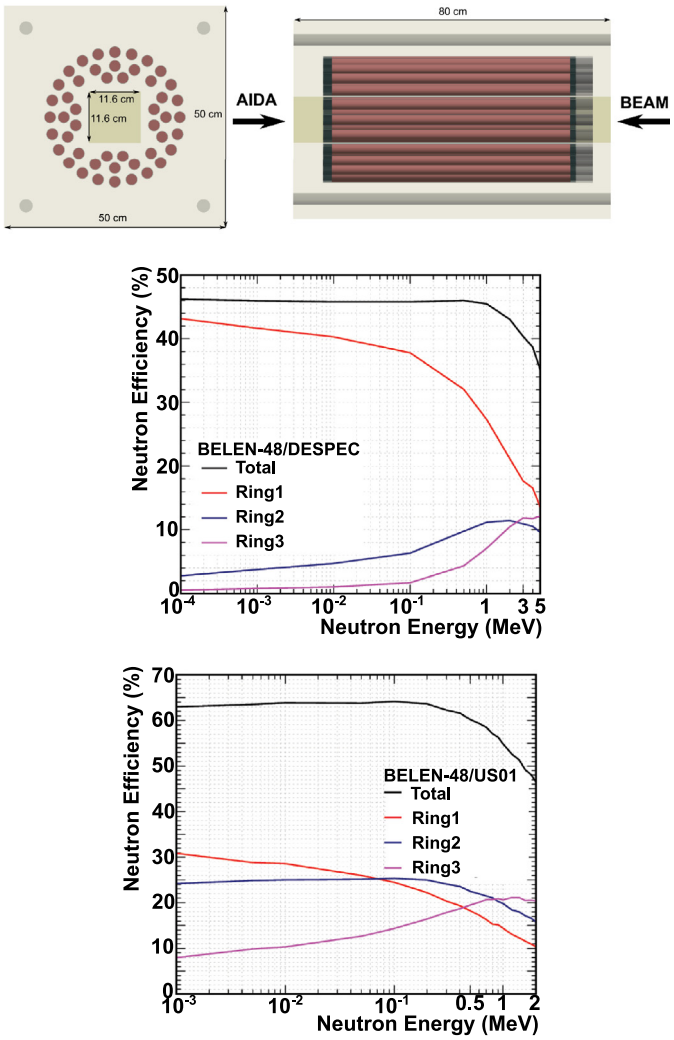

Fig. 9. Upper panel: Schematic of the cross and lateral section of polyethylene matrix where the ^{3}He proportional counters are shown in red. Middle/lower panels: Neutron detection efficiency for BELEN-48 detectors up to 5 MeV, obtained by Monte Carlo simulations with MCNPX, in the standard configuration (middle) and optimised for low $Q_{\beta n}$ windows (lower). See text for details.

2.6. BELEN

The BEta-deLayEd Neutron (BELEN) [16] detector is a moderated neutron counter for the measurement of neutron emission probabilities after β-decay (β-delayed neutrons). The BELEN detector consists of an array of proportional neutron counters, embedded into a High Density PolyEthylene (HDPE) moderator surrounding an implantation detector. The neutron detection in the proportional counters exploits the large cross section for thermal neutrons of the reaction $^{3}\mathrm{He} + n_{th} \rightarrow {}^{1}\mathrm{H} + {}^{3}\mathrm{H}$ (+ 765 keV), in order to achieve an overall high detection efficiency. The polyethylene moderator plays a major role reducing the higher energy β-delayed neutrons down to the thermal region. The design concept behind the BELEN detector is to achieve a maximum neutron detection efficiency as independent as possible from the neutron energy (flat efficiency). A flat efficiency means that systematic effects on the determination of the β-delayed emission probability due to the unknown energy spectrum of β-delayed neutrons are avoided. There are two versions of BELEN-48 specially designed to be used with AIDA for the DESPEC experiment at FAIR. In both versions, the 48 ^{3}He-tubes are distributed in three concentric rings embedded in a moderator core of size 50 × 50 × 80 cm^{3}. An extra HDPE moderator piece (20 cm thickness) is placed surrounding the core and used as a shielding for background neutrons.

The BELEN-48/DESPEC version is intended for the measurement of nuclei with large $Q_{\beta n}$ windows (see middle panel of Fig. 9). In this case, the moderator has a central hole of 16 cm diameter which provides some flexibility for the configuration of the implantation detector with other ancillary systems. The impact of this design is shown in Fig. 9 middle panel, with a flat neutron efficiency (45%) for 100 keV–1 MeV. BELEN-48/US01 is an alternative high efficiency version with a square shaped central hole of 11.6 cm side. In Fig. 9 lower panel, a flat neutron efficiency (65%) is achieved from 100 keV up to 500 keV. This detector design is useful for experimental cases involving low $Q_{\beta n}$ windows, when the expected neutron emission energies are concentrated below 500 keV.

BELEN-30 was used at GSI for the first measurement of β-delayed neutron emitters beyond $N = 126$ [49]. An earlier version of the detector was used in measurements at the IGISOL IV facility in Jyväskylä [50].

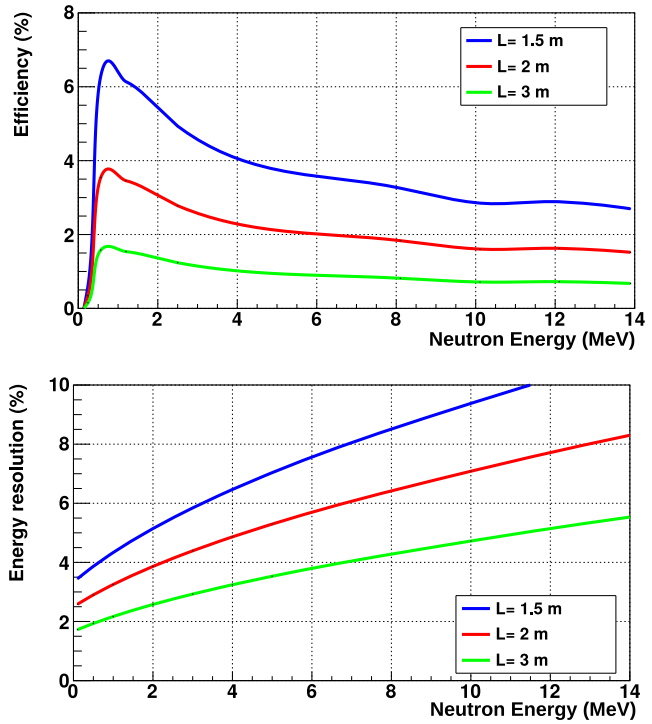

Fig. 10. Upper panel: Total efficiency for full array setup (100 detectors) for a flight distance of 1.5, 2 and 3 m. Bottom panel: Energy resolution estimated for different flight distance assuming an overall time resolution of 1.5 ns and a 2.5 cm uncertainty in the flight path reconstruction.

2.7. MONSTER

The MOdular Neutron SpectromeTER (MONSTER) [17] will be employed for the determination of the energy spectra of β-delayed neutrons and their partial branching ratios to the excited states in the final nucleus by applying $\beta - \gamma$-n coincidences. The neutron energy is determined by the time-of-flight technique, thus the spectrometer must be used in combination with a fast β-detector to provide a start-up signal. In DESPEC, the βPlastic detector will provide the start signal with an excellent time resolution and reasonable efficiency.

The neutron spectrometer consists of cylindrical cells of 200 mm diameter and 50 mm height, filled with BC501 A or EJ301 scintillating liquid. Each cell is coupled through a light guide of 31 mm thickness to R4144 or R11833 PMT models. Details of the design can be found in Refs. [17,51]. The full spectrometer will consist of up to 100 cells placed at a flight distance that takes into account the trade-off between efficiency and energy resolution required for each experimental measurement. The configuration of the spectrometer array can be easily customised according to the number of detectors and flight distance needed for each experiment, thanks to the aluminium profile rack-type stands used for the mechanical structure.

The detector response has been characterised both experimentally with mono-energetic neutron beams, and by Monte Carlo simulations. The total efficiency has been determined for the full spectrometer placed at different flight distances, with a threshold of 30 keVee (electron equivalent) – see Fig. 10. The energy resolution has been calculated for a realistic total time resolution of 1.5 ns and assuming 2.5 cm as uncertainty in the flight distance.

A reduced version of MONSTER with 48 detectors was used to measure the delayed neutron emission in the decay of ^{85}As at JYFL in early 2019 as a first commissioning run, and a four-detector set was employed close to the DESPEC setup during a short commissioning run later in 2019, to study the background in the experimental area. Examples of the modules and the aluminium holding structure are shown in Fig. 11.

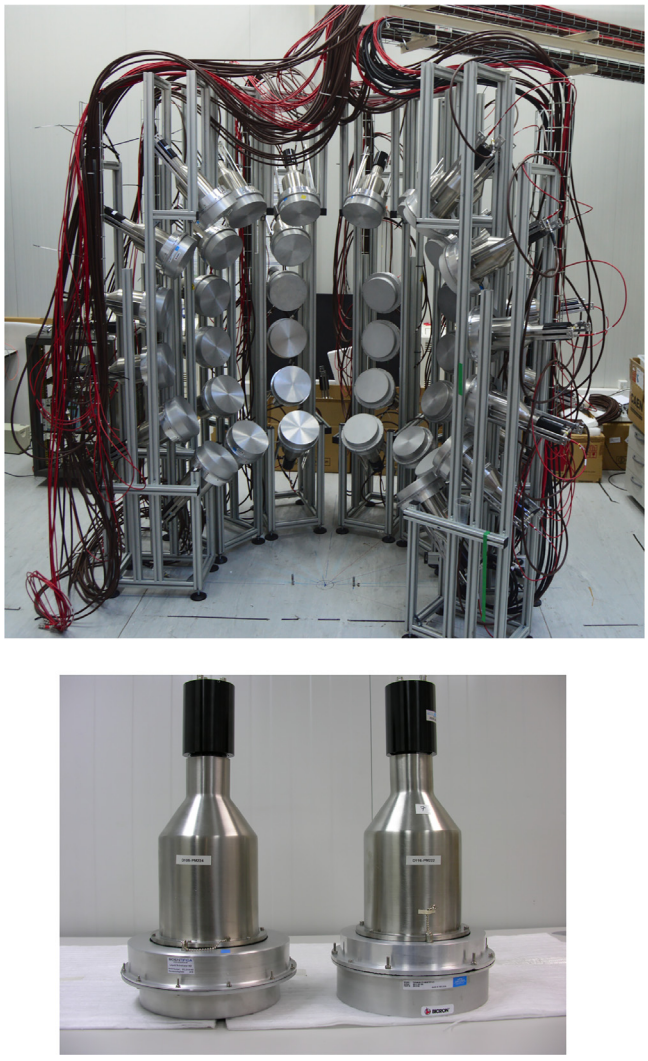

Fig. 11. Upper photograph: MONSTER array characterisation setup at Centro de Investigaciones Energéticas Medioambientales y Tecnológicas (CIEMAT). The detector cells are placed in the holding structure. Lower photograph: Two individual MONSTER detector cells.

3. Data infrastructure and processing

The DESPEC setup consists of a range of individual subsystems, and therefore requires a complex data acquisition framework. The key requirements include an integration of the various components and minimisation of the dead time. The DESPEC objective is to follow the general NUSTAR DAQ (or NDAQ) concept, described in the NDAQ TDR [52]. The details provided here apply to the common aspects of the overall system. An example of a schematic of a typically employed arrangement is given in Fig. 12.

3.1. MBS

The DESPEC subsystems (excluding AIDA and MONSTER) use the GSI-developed Multi-Branch-System (MBS) [55]. Each individual subsystem has its own MBS DAQ, which are then merged using a timesorter event builder. For events to be correlated using the White Rabbit timing [56], the additional step of unpack and check every single bit (ucesb) is required (see below). The timesorter requires all connected DAQs to be responding and continuously sending data. This is achieved with a synchronisation pulser (2 Hz) and requires active monitoring of the subsystem DAQs. The data in list mode format are stored to tape

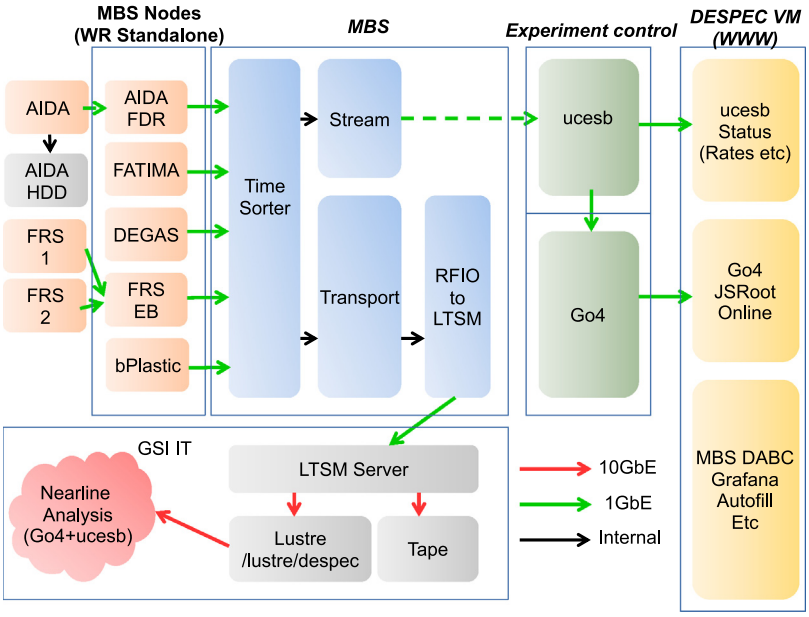

Fig. 12. Example of a typical DESPEC DAQ architecture. Data from the individual subsystems (orange squares on the left) are fed into a timesorter for event building. From the stream server branch they are sent to the ucesb timesticher which serves to stitch subevents based on the White Rabbit common clock. From there the data are streamed to the Go4 on-line analysis, both ucesb and Go4 are linked to the World Wide Web via the Apache fastCGI webserver [53]. From the transport server they are stored to magnetic tape and to the Lustre file server, in parallel, via Lightweight Tivoli Storage Manager(LTSM) [54]. From Lustre, the data can be accessed for near-line analysis on the GSI cluster computing service in batch-mode processing.

and, in parallel, to the GSI Lustre file server via the Lightweight Trivoli Storage Manager(LTSM) [54].

3.2. Event timestamping

The global synchronisation of the various DESPEC subsystems is achieved using White Rabbit timing, which will be the standard at the future FAIR facility. Further information regarding White Rabbit can be found in Ref. [56]. The White Rabbit timing epoch (absolute start time) is midnight on January 1st, 1970, and is driven by a 125 MHz clock and distributed to the DESPEC subsystems via Ethernet. The timestamp accuracy can be up to ∼1 ns and depends on the type of receiving board. The VME systems (FRS and FATIMA-VME) use the VETAR2 timing boards, which provide an 8 ns timestamp accuracy. The FEBEX (HPGe) and TAMEX (βPlast and FATIMA-TAMEX) systems employ a PCI-Express To Optical Link Interface (PEXARIA) receiver [57], resulting in 1 ns accuracy. AIDA connects to the White Rabbit system via HDMI cable from a VME Timing Receiver for White Rabbit (VETAR2) [58] or PEXARIA receiver. A timestamp precision of 10 ns is available for the FEBEX system used with the germanium detectors. In addition, a CFD mode is implemented wherein an additional interpolation of the zero crossing allows for <10 ns timing resolution.

The MONSTER DAQ runs in triggerless mode although a triggered version is also available. In addition, the DAQ has been designed to run in standalone mode, or to be merged with the rest of the DESPEC DAQ subsystems. This is achieved using a 10 MHz clock and an external synchronisation signal for a time-stamping mark [59].

For DTAS and BELEN, the self-triggered digital data acquisition system GASIFIC-7.0 [60] is used to register DTAS signals. It is based on Struck SIS3316 digitiser cards. In order to integrate this system into the DESPEC DAQ (see Section 3) the White Rabbit signal will be encoded within the 200 MHz clock pulses produced by a VETAR2 module, which is then plugged as external clock to the SIS3316 modules. New firmware has been developed by Struck in order to decode and insert the WR timing in the digitiser data stream.

To ensure constant synchronisation of the multiple subsystems, a module was developed that generates two output pulses for every input pulse. The output pulses have one with minimal delay and one with a variable delay. Upon activation, the pulse with variable delay occurs with no delay with respect to the pulse with minimal delay, but the delay of each subsequent pulse increases by an additional 50 ns. In this way, the output of the variable delay for the Nth pulse occurs a total of (N-1)*50 ns after the minimally-delayed output. After 32 (or 64) repetitions, the cycle ends and the delay becomes 0 ns again. Each subsystem receives a copy of the minimally-delayed output and the variable-delay output. In this way, the synchronisation between subsystems can be verified by investigating the time difference between the two signals.

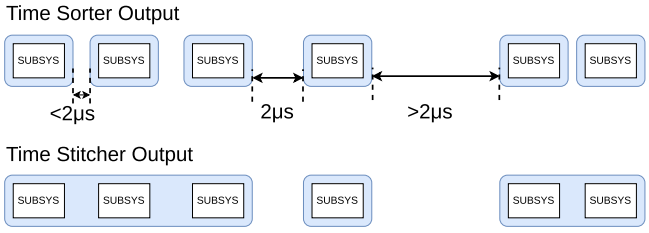

Fig. 13. Schematic of the ucesb time-stitching algorithm. Events from subsystems occurring less than a defined time (normally 2 μs) from the previous event are grouped together. Events themselves are unmodified.

3.3. Timestitching with ucesb

"Unpack and check every single bit" (ucesb) [62] is a general-purpose data unpacker with powerful MBS processing capabilities. For DESPEC, ucesb is used as an MBS post-processor to build AIDA events and to time-stitch the data for subsequent analysis. It also functions as a 'FIFO' server allowing many clients to connect to the online data at once. The time-stitching process combines 'near' events from different subsystems into a single MBS event, such that all the different subsystem data may be accessed at once in subsequent analysis and ROOT trees generation [63], simplifying the task considerably. The algorithm to combine events operates by looking for a gap in time to break up events: this is largely based on AIDA's high self-trigger rate

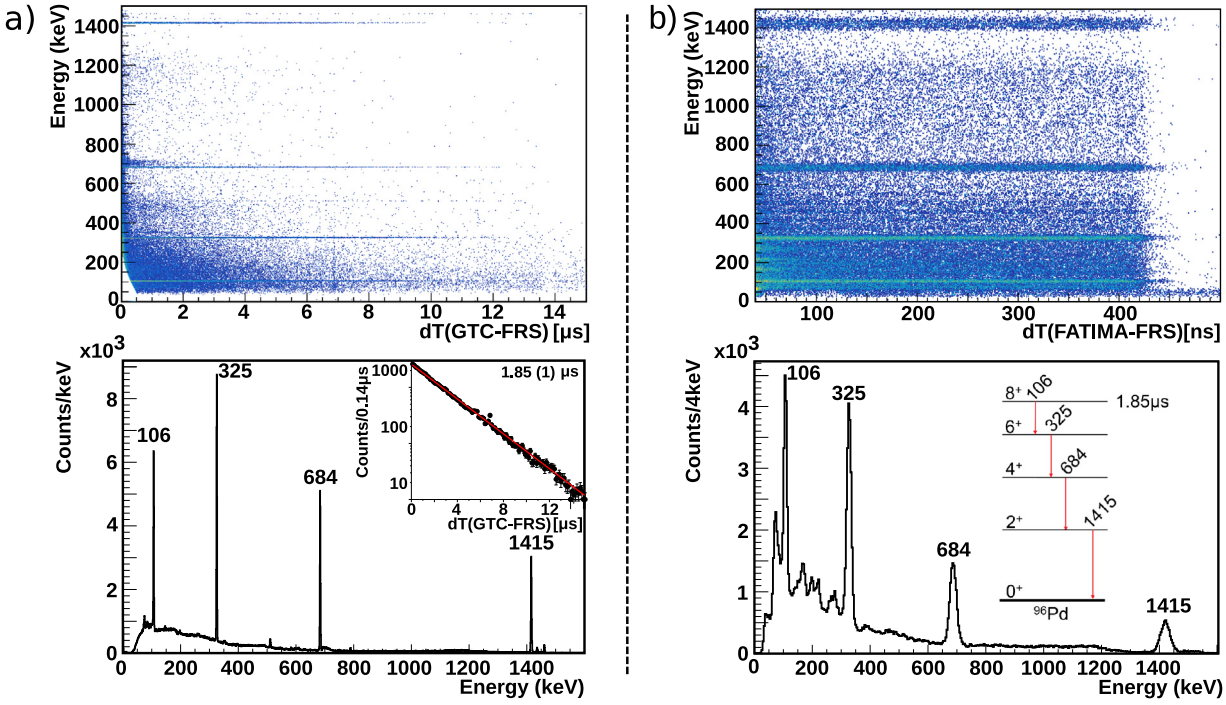

Fig. 14. (a) Prompt GTC spectra obtaining during Exp.# 2 correlated with ^{96}Pd ions in the FRS. Top: Energy vs. time difference between signals from the GTC and from the S4 scintillator in the FRS. (>2 counts/bin for clarity). Bottom: Projected γ-ray energy spectrum from top, in the inset the half-life extracted of 1.85(1) μs after gating on the 106, 325, 684 and 1415 keV γ-ray lines. (b) Same as (a) but for FATIMA. Note that the short collection time window for FATIMA restricts the ability to extract the ≈2 μs isomer decay half-life for this particular study. The level scheme collated in [61] is shown as an inset in the lower panel of (b).

and its internal multiplexing. At present, the algorithm combines events until a gap of 2 μs is observed between events, shown in Fig. 13.

3.4. Data monitoring and near-line analysis

The quality of the incoming data is monitored using software based on the GSI developed Go4 [64] analysis based in ROOT [63]. With the online software one can monitor the incoming data in real-time to keep track on individual subsystems.

The Data Acquisition Backbone Core (DABC) framework [65] enables the online DAQ rates to be accessible via the World Wide Web via the Apache fastCGI webserver [53]. This was particularly relevant for remote access during the COVID19 crisis, in order to continue experimental campaigns where only a limited team was available on-site. The monitoring of the (near) real-time histograms is done both on-site locally, and is available through the World Wide Web using the JSROOT development [66], which acts to unpack the DABC objects.

The volume of incoming data is relatively large (experiment dependent, but up to 100MB/s). Since this data rate is computationally challenging to process in real time, a near-line sort was developed in parallel, such that the full data set can be analysed in a relatively short time. To process the large data volumes, the GSI high-performance computing cluster is utilised [67]. This utilises the Slurm Workload Manager [68] such that list mode data files can be submitted in parallel and merged after being sorted.

The long-term goal will be to produce software based on the FairRoot development [69], which will be the standard framework of physics data monitoring, analysis and simulations for the FAIR project.

4. First applications and analysis

A campaign of commissioning and day-one experiments was performed using the DESPEC setup during 2019–2021. A selection of results introducing the capabilities of the device is described in the following subsections, along with the given setup employed. The studies

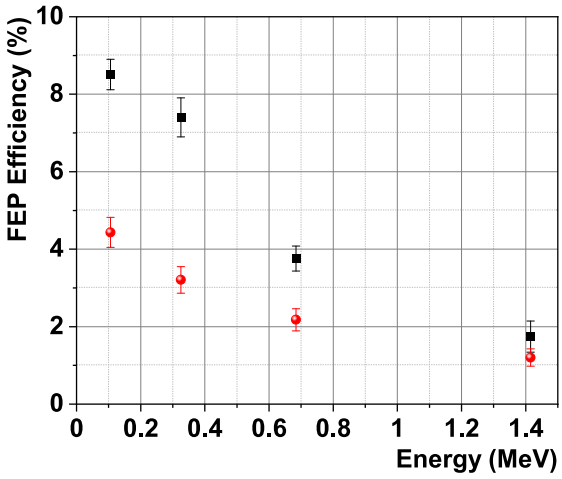

Fig. 15. Full energy peak efficiency measured in Exp.# 2, obtained from γ singles to $\gamma-\gamma$ coincidence ratios for FATIMA (black squares) and GTC (red circles).

were used both to test the single detectors, their electronics, and to fully integrate all the subsystems together in the same DAQ environment. In addition the goal was to obtain physics measurements as part of the FAIR Phase-0 program. Nuclei with previously reported isomeric states and/or β-decay branches were used to check the on-line and off-line analysis programs and define best working conditions to ensure ion-γ and ion-$\beta-\gamma$ correlations. Further results from these studies will be detailed in future dedicated publications.

For 2019/2020, one configuration involved coupling AIDA to the FATIMA fast-timing array and additional high-resolution HPGe detectors, GALILEO triple clusters (GTC). The GTC detectors were placed at 280 mm from the centre of the DSSD stack and the FATIMA detectors

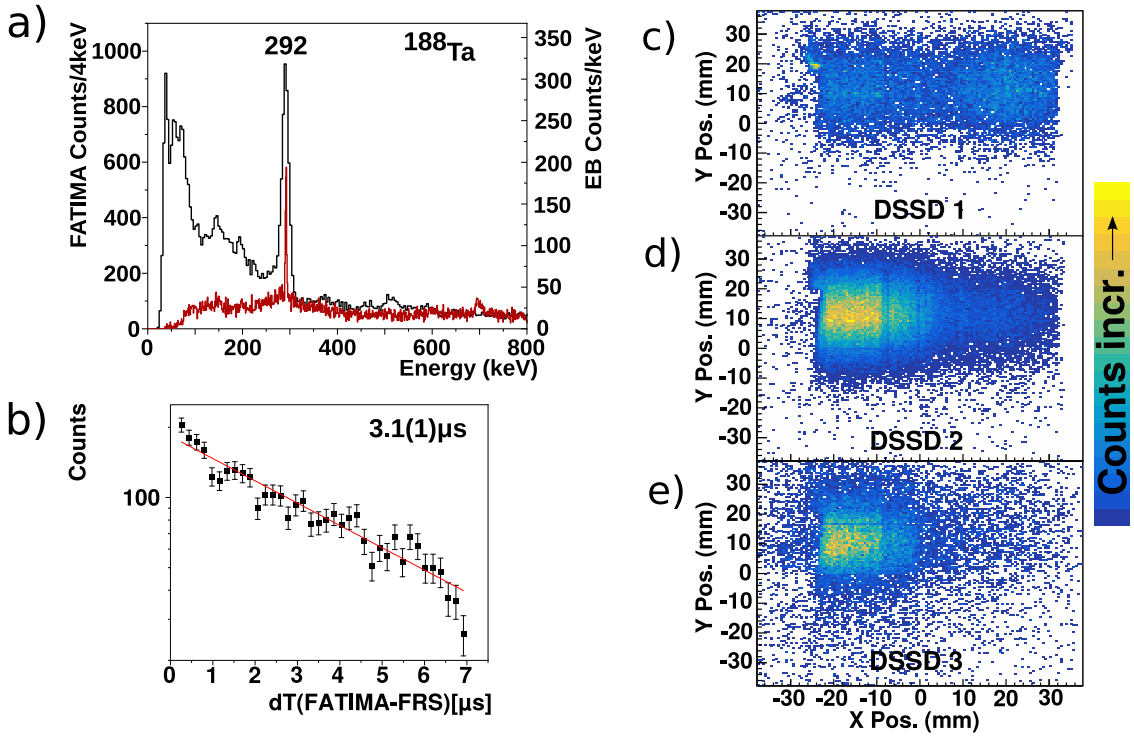

Fig. 16. (a) Coincident γ-ray energy spectra detected by FATIMA (black) and EB (red) detectors after applying gating conditions to the FRS particle identification on ^{188}Ta ions. (b) The isomeric half-life of 3.1(1) μs obtained with dT(FATIMA-FRS) after coincidence gating on the 292 keV γ-ray line. Spectra (c)–(e) show stopped ^{188}Ta ions in the AIDA DSSDs 1–2 and all ions in DSSD 3, respectively.

Table 1
List of experiments for reference in chronological order discussed in this article. (GTC — Galileo Triple Cluster, EB — EUROBALL 7-fold Cluster).

Exp.#	Date	This work	Config.
1	2019	^{34}Si	FATIMA
2	2020	^{96}Pd,^{94}Ru	FATIMA+GTC
3	2021	^{188}Ta	FATIMA+2 EB Cluster

are at 160 mm. For 2021 the GTC detectors were replaced by EUROBALL 7-fold cluster germanium detectors (EB). Table 1 gives a reference list of the experiments, deployed setup configuration, and synthesised nuclei evaluated in this work to demonstrate the performance of the setup.

4.1. Ion-isomer correlations: ^{96}Pd and ^{188}Ta cases

^{96}Pd is known to have an $I^{\pi}= 8^{+}$ seniority isomer with a 2.1 μs mean half-life (see for example [70–74]). To observe ion-γ correlations, during Exp.# 2, ^{96}Pd was produced using a ^{124}Xe fragmentation reaction and implanted into AIDA. More than 10^{6} ^{96}Pd implanted ions were identified.

The DAQ collection windows were set to 0–20 μs and 0–400 ns, for the GTC and FATIMA respectively. The FRS scintillator signal in the S4 focal plane was sent to both the FATIMA and the GTC DAQs for efficient ion-γ time correlations. To enhance the γ-ray decay lines over the prompt radiation flash and background, γ rays arriving in a delayed interval of dT(FATIMA-FRS) = 40–400 ns and dT(GTC-FRS) = 0–12 μs after the start of the event were considered. An additional cut on a 2D matrix of the energy vs. dT(GTC-FRS) for the prompt radiation flash was applied for the GTC detectors.

In Fig. 14 delayed γ rays in coincidence with ^{96}Pd ions selected in the FRS are shown for the GTC 14(a) and FATIMA 14(b) detectors. Gamma-ray transitions following the decay of the 8^{+} isomeric state are clearly visible in the spectra. The additional lines in the FATIMA spectrum in the range 150–280 keV stem from a neutron inelastic scattering $(n, n'\ \gamma)$ [75]. The measured energy resolution in FATIMA and the GTC detectors at 1415 keV was determined to be on average 3% and 0.2% (FWHM), respectively. The fit to the single exponential decay in 14a) yields a half-life of 1.85(1) μs thus is consistent with, but more precise than the value given in [73] (1.75(6) μs) and the mean value across several measurements in [61] (2.1(21) μs), due to enhanced statistics.

The full energy peak efficiency of FATIMA and the GTC was determined by taking the ratio of counts between the $\gamma-\gamma$ coincident gated γ rays, and the singles γ-ray counts (corrected for internal conversion). This is shown in Fig. 15. These results helped to validate a GEANT4 simulation of the array detailed in [76]

A separate experimental run (Exp.# 3) was devoted to the study of ion-isomer correlations in a heavier region of the nuclide chart, around ^{188}Ta produced in a fragmentation reaction with a ^{208}Pb primary beam. In this case, the Euroball 7-fold germanium clusters (EB) were employed. An example of FRS ion-AIDA correlations is shown in Fig. 16. By selecting (i.e. coincidence gating) the ^{188}Ta ions identified in the FRS, the γ-rays in coincidence can be identified and thus the isomer can be extracted which depopulates via a 292 keV γ-ray transition (Fig. 16a)) with a measured half-life $T_{1/2}$ = 3.1(1) μs (Fig. 16b)). This is consistent with the value reported in [77] ($T_{1/2}$ = 3.7(4) μs).

Fig. 16(c) and (d) show the coincidence between ^{188}Ta ions in the FRS and the AIDA DSSDs, with a condition on DSSD 1 and DSSD 2 that no ion is observed in a further downstream DSSD within a given event (i.e. the ion is stopped). As there is no further downstream detector to DSSD3, Fig. 16(e) shows the distribution of all coincident gated ^{188}Ta ions in DSSD 3, stopped or traversing through the detector. The conditions on all three DSSDs ensure that the ions are correctly implanted into the expected position, which is in turn used for ion-γ (isomers) and $\beta-\gamma$ correlations.

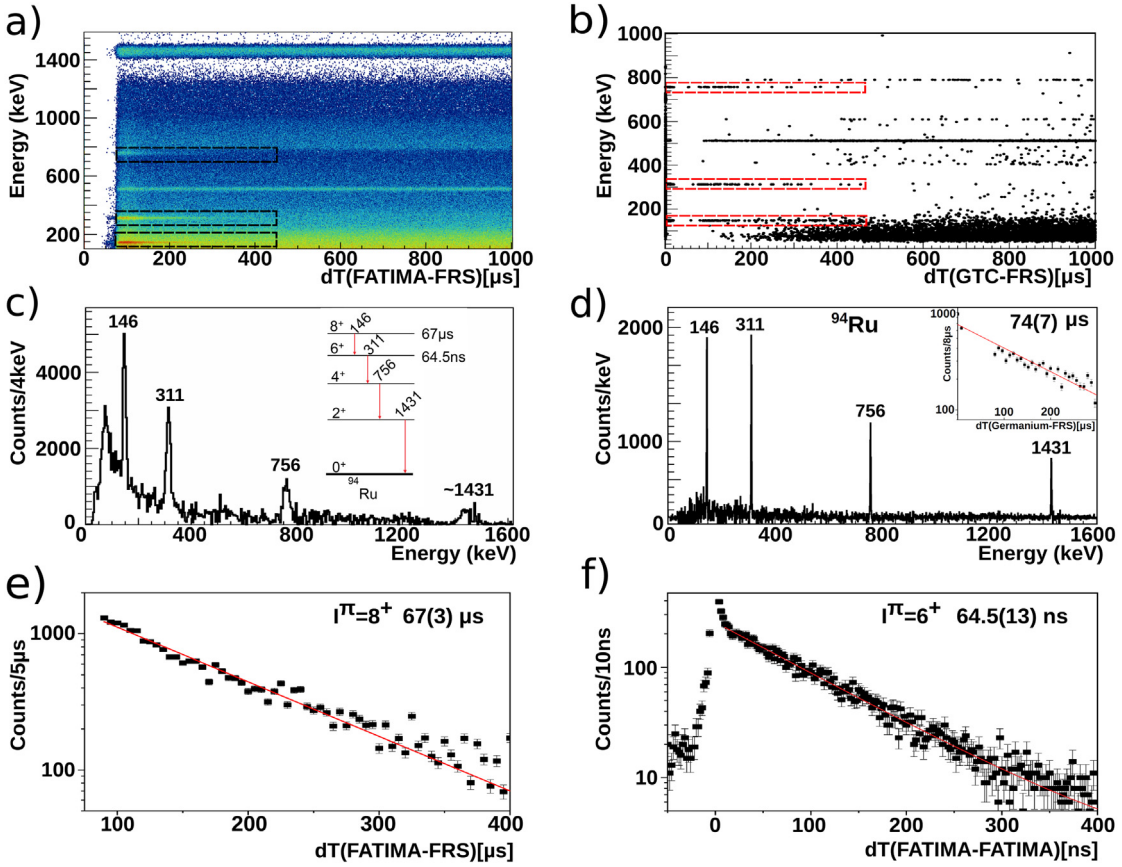

Fig. 17. Gamma-rays in coincidence with ^{94}Ru ions in the FRS. (a) FATIMA energy vs. FATIMA-Ion time difference and (b) GTC energy vs. GTC-FRS dT. The transitions of interest are marked in the black (a)) and red (b)) dashed boxes to guide the eye (146 keV, 311 keV, 756 keV). c)Left panel: FATIMA γ rays within the time period dT(FATIMA-FRS(^{94}Ru)) = 0–1 ms, with a normalised background subtraction applied from the time region 1 ms–2 ms. Right panel: level scheme as taken from [61] (d) GTC γ-ray energy within the time period dT(GTC-FRS(^{94}Ru)) = 0-1 ms, with a normalised background subtraction applied from the time region 1 ms–2 ms. In the inset, the extracted isomeric halflife is 74(7) μs. (e) relatively longer lived 8^+ isomer as extracted from FATIMA-FRS in coincidence with the 146, 311, and 756 keV γ-ray lines including background subtraction. (f) relatively shorter lived 6^+ isomer extracted using delayed FATIMA $\gamma-\gamma$ coincidences with the 311 and 756 keV γ-ray transitions.

4.2. Longer ion-isomer correlations: ^{94}Ru isomeric decays

^{94} Ru has a previously reported 71(5) μs isomer [78] stemming from the $I^{\pi}=8^+$ seniority isomer. In our work, ^{94}Ru was produced as a fragment reaction channel in Exp.# 2.

Using the White Rabbit timing between FRS and GTC/FATIMA events, it is possible to extract the γ rays beyond the standard DAQ time windows. This was done by opening a time window dT(γ-FRS) 0-1 ms after the detection of a ^{94}Ru ion in the FRS and AIDA (stopped), and collating all γ rays in this time frame as plotted in Figs. 17(a) and (b). Here, the electronics dead time of the systems can be seen with ≈400 ns–70 μs dead time for FATIMA (prompt collection time window 0–400 ns) and ≈20 μs–60 μs for GTC (prompt time window 0-8 μs).

The normalised background-subtracted energy projections are shown in 17(c) and (d). From the two figures, the γ-ray lines corresponding to ^{94}Ru are clearly visible.

In addition, the isomeric half-lives can be extracted as shown in Fig. 17(e) for FATIMA, and the inset in Fig. 17(d) for the GTC. The dT(γ-FRS) time window was selected as 0-450 μs (i.e. ≈6× $T_{1/2}$) with coincidence gates on the 146, 311, and 756 keV γ-ray lines. Note that the 1431 keV line is a doublet in FATIMA due to the electron capture decaying ^{138}La → ^{138}Ba which populates an excited $I^{\pi}=2^+$ state and subsequently decays via a 1436 keV γ-ray transition. The $T_{1/2}$=67(3) μs half life extracted from the minimisation fit is in agreement with the value given in [78].

For the $I^{\pi}=6^+$ state, which is populated in decays of the longer lived $I^{\pi}=8^+$ state, the relatively shorter isomeric decay (< the collection window time) can be extracted by using the energy coincidence gated time differences between detectors in FATIMA as shown in Fig. 17f). The $T_{1/2}$=64.5(13) ns half-life of the $I^{\pi}=6^+$ state is measured by using the dT between FATIMA detectors by coincidence gating on the 311 keV (start) and 756 keV (stop) transitions. The isomeric half-life obtained here is in agreement with the value measured in Ref. [79] (65(2) ns) and the γ-ray energies are in agreement with [80].

4.3. Beta-delayed γ rays: the decay of ^{34}Si → ^{34}P

The DESPEC setup is designed to measure γ rays from levels populated by β decay. For this, a combination of FRS, AIDA and γ-ray detectors are required. This can be achieved using a multi-fold coincidence as follows:

(i) coincidence gating on the ion in the FRS (see e.g. Fig. 16),
(ii) selecting the implant in AIDA on a pixel by pixel basis,
(iii) observing a decay in AIDA within a certain front–back matched DSSD energy and time condition, and maximum energy condition within a cluster of pixels surrounding the implanted ion pixel,
(iv) applying a time gate between the implanted ion and subsequent β decay.

As an example of this, γ rays following the β^-decay of ^{34}Si → ^{34}P are shown in Fig. 18. The conditions applied were: ^{34}Si FRS ion gated, dT(implant-decay)=0–10 s, White Rabbit gate between AIDA

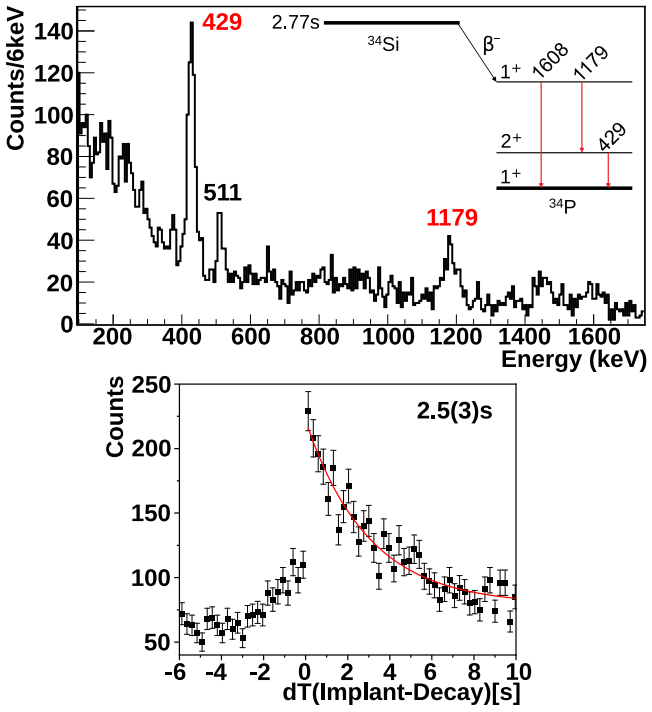

Fig. 18. Upper panel: Beta-delayed γ rays in FATIMA correlated with an ion from the FRS, implant into AIDA and subsequent decay within 10 s. See text for correlation conditions. Inset: the level scheme established in [81]. Lower panel: Implant-decay time difference. From an exponential fit to the decay curve, a half-life of 2.5(3) s was extracted.

and FATIMA, energy (>200 keV) and time cuts for the β decays in AIDA, a punchthrough veto for ions using the downstream β-plastic detector, AIDA decay multiplicity cut <10 and a 50 μs veto from the scintillator at S4. Note that during this experiment only the FATIMA array was available.

The γ-ray energies following these conditions can be seen as the 1179 and 429 keV in Fig. 18 upper panel, corresponding to the $I^{\pi}= 1^{+} \rightarrow 2^{+}$ and $2^{+} \rightarrow 1^{+}$ transitions respectively (see inset level scheme). The β-decay half-life extracted from the implant-decay time (Fig. 18 lower panel) is in agreement with the value given in [81].

5. Summary and outlook

The DESPEC setup discussed in this work has been developed for the FAIR Phase-0 project and for first day-one experiments at the new facility. A successful commissioning campaign has demonstrated the capabilities of the initial hybrid setup including ion-γ, and ion-$\beta - \gamma$ correlations using the FATIMA array coupled to HPGe detectors. In addition, a suite of newly designed and constructed detector systems allows for a comprehensive and expansive physics program to be performed with the overall goal of addressing outstanding questions in nuclear structure physics. For the future, new developments are planned to optimise the setup in view of deployment at the low energy branch of the Super-FRS. Such developments are not limited to, but include for example: Machine learning algorithms for βPlastic position information, BGO shields developed to suppress the Compton background of the DEGAS array, upgrades to the online and offline analysis within the FairRoot framework, and comprehensive simulation software developments in GEANT4 (for which work has already begun). A campaign of measurements is planned with DESPEC for 2022 at GSI in a continuation of the experimental program in the framework of FAIR Phase-0.

CRediT authorship contribution statement

A.K. Mistry: Writing – original draft, Analysis, Software. **H.M. Albers:** Writing – original draft, Analysis. **T. Arıcı:** Writing – original draft, Hardware. **A. Banerjee:** Writing – original draft, Hardware. **G. Benzoni:** Project administration, Conceptualization. **B. Cederwall:** Supervision. **J. Gerl:** Project administration, Conceptualization. **M. Górska:** Project administration, Conceptualization. **O. Hall:** Investigation, Hardware. **N. Hubbard:** Writing – original draft, Software, Analysis. **I. Kojouharov:** Writing – original draft, Hardware. **J. Jolie:** Supervision. **T. Martinez:** Writing – original draft, Hardware. **Zs. Podolyák:** Writing – original draft, Supervision. **P.H. Regan:** Supervision, Conceptualization. **J.L. Tain:** Writing – original draft, Conceptualization. **A. Tarifeno-Saldivia:** Writing – original draft. **H. Schaffner:** Writing – original draft, Hardware. **V. Werner:** Supervision. **G. Ağgez:** Investigation. **J. Agramunt:** Investigation. **U. Ahmed:** Investigation. **O. Aktas:** Investigation. **V. Alcayne:** Investigation. **A. Algora:** Investigation. **S. Alhomaidhi:** Investigation. **F. Amjad:** Investigation. **C. Appleton:** Investigation. **M. Armstrong:** Investigation. **M. Balogh:** Investigation. **K. Banerjee:** Investigation. **P. Bednarczyk:** Investigation. **J. Benito:** Investigation. **C. Bhattacharya:** Supervisor. **P. Black:** Hardware. **A. Blazhev:** Investigation. **S. Bottoni:** Investigation. **P. Boutachkov:** Investigation. **A. Bracco:** Investigation. **A.M. Bruce:** Investigation. **M. Brunet:** Investigation. **C.G. Bruno:** Investigation. **I. Burrows:** Hardware. **F. Calvino:** Investigation. **R.L. Canavan:** Investigation. **D. Cano-Ott:** Project administration. **M.M.R. Chishti:** Investigation. **P. Coleman-Smith:** Hardware. **M.L. Cortés:** Investigation. **G. Cortes:** Investigation. **F. Crespi:** Investigation. **B. Das:** Investigation. **T. Davinson:** Investigation. **A. De Blas:** Investigation. **T. Dickel:** Investigation. **M. Doncel:** Investigation. **A. Ertoprak:** Investigation. **A. Esmaylzadeh:** Investigation. **B. Fornal:** Investigation. **L.M. Fraile:** Investigation. **F. Galtarossa:** Investigation. **A. Gottardo:** Investigation. **V. Guadilla:** Investigation. **J. Ha:** Investigation. **E. Haettner:** Investigation. **G. Häfner:** Investigation. **H. Heggen:** Hardware. **P. Herrmann:** Investigation. **C. Hornung:** Investigation. **S. Jazrawi:** Investigation. **P.R. John:** Investigation. **A. Jokinen:** Supervision. **C.E. Jones:** Investigation. **D. Kahl:** Investigation. **V. Karayonchev:** Investigation. **E. Kazantseva:** Investigation. **R. Kern:** Investigation. **L. Knafla:** Investigation. **R. Knöbel:** Investigation. **P. Koseoglou:** Investigation. **G. Kosir:** Investigation. **D. Kostyleva:** Investigation. **N. Kurz:** Hardware. **N. Kuzminchuk:** Investigation. **M. Labiche:** Hardware. **J. Lawson:** Hardware. **I. Lazarus:** Hardware. **S.M. Lenzi:** Investigation. **S. Leoni:** Investigation. **M. Llanos-Expósito:** Investigation. **R. Lozeva:** Investigation. **A. Maj:** Supervision. **J.K. Meena:** Investigation. **E. Mendoza:** Investigation. **R. Menegazzo:** Investigation. **D. Mengoni:** Investigation. **T.J. Mertzimekis:** Investigation. **M. Mikolajczuk:** Investigation. **B. Million:** Investigation. **N. Mont-Geli:** Investigation. **A.I. Morales:** Investigation. **P. Morral:** Hardware. **I. Mukha:** Investigation. **J.R. Murias:** Investigation. **E. Nacher:** Hardware. **P. Napiralla:** Investigation. **D.R. Napoli:** Supervision. **B.S. Nara-Singh:** Investigation. **D. O'Donnell:** Hardware. **S.E.A. Orrigo:** Investigation. **R.D. Page:** Investigation. **R. Palit:** Investigation. **M. Pallas:** Investigation. **J. Pellumaj:** Investigation. **S. Pelonis:** Investigation. **H. Pentilla:** Investigation. **A. Pérez de Rada:** Investigation. **R.M. Pérez-Vidal:** Investigation. **C.M. Petrache:** Investigation. **N. Pietralla:** Supervision. **S. Pietri:** Investigation. **S. Pigliapoco:** Investigation. **J. Plaza:** Investigation. **M. Polettini:** Investigation. **C. Porzio:** Supervision. **V.F.E. Pucknell:** Hardware. **F. Recchia:** Investigation. **P. Reiter:** Project administration. **K. Rezynkina:** Investigation. **S. Rinta-Antila:** Investigation. **E. Rocco:** Investigation. **H.A. Rösch:** Investigation. **P. Roy:** Investigation. **B. Rubio:** Investigation. **M. Rudigier:** Investigation. **P. Ruotsalainen:** Investigation. **S. Saha:** Investigation. **E. Şahin:** Investigation. **Ch. Scheidenberger:** Supervision. **D.A. Seddon:** Hardware. **L. Sexton:** Investigation. **A. Sharma:** Investigation. **M. Si:** Investigation. **J. Simpson:** Supervision. **A. Smith:** Hardware. **R. Smith:** Hardware. **P.A. Söderström:** Investigation. **A. Sood:** Investigation. **A. Soylu:** Investigation. **Y.K. Tanaka:**

Investigation. **J.J. Valiente-Dobón:** Investigation. **P. Vasileiou:** Investigation. **J. Vasiljevic:** Investigation. **J. Vesic:** Investigation. **D. Villamarin:** Investigation. **H. Weick:** Investigation. **M. Wiebusch:** Hardware. **J. Wiederhold:** Investigation. **O. Wieland:** Investigation. **H.J. Wollersheim:** Supervision. **P.J. Woods:** Project administration. **A. Yaneva:** Investigation. **I. Zanon:** Investigation. **G. Zhang:** Investigation. **J. Zhao:** Investigation. **R. Zidarova:** Investigation. **G. Zimba:** Investigation. **A. Zyriliou:** Investigation.

Declaration of competing interest

The authors declare that they have no known competing financial interests or personal relationships that could have appeared to influence the work reported in this paper.

Acknowledgements

We would like to acknowledge the excellent work of the GSI accelerator department. Thanks go to Dr. B. Löher for his support and assistance with DAQ and ucesb related matters. PHR, ZP and MMRC were supported by the UK STFC UK Nuclear Data Network and the UK STFC via Grants No. ST/L005743/1 and No. ST/P005314), RLC was supported by an award from the Marion Redfearn Trust, P.H.R. acknowledges support from the UK Government Department of Business, Energy, and Industrial Strategy via the National Measurement System. J.J., A.B., A.E., V.K., P.K., L.K., V.W. acknowledge support by the BMBF-Rahmenprogramms ErUM Verbundsprojekt ErUM-FSP T07, Germany grant 05P19PKFNA, 05P21RDFNA, 05P21RDFN1, 05P19RDFN1 and 05P21PKFN1. R.L., M.S., G.H. acknowledge support by IN2P3-GSI collaboration agreements 18–78 France on GSI/FAIR. This work was supported by the Swedish Research Council under Grants No. 621-2014-5558 and 2019-04880. J.B, L.M.F., M.L.-E., and J.R.M. acknowledge funding through the Spanish government via project number RTI2018-098868-B-I00. Work at JSI was supported by the Slovenian research agency grants No. I0-0005 and P1-0102. A.Z. was supported by the Hellenic Foundation for Research and Innovation (HFRI), Greece under the HFRI PhD Fellowship grant (Fellowship Number: 101742/2019). R.D.P. and D.A.S. were supported by the U.K. Science and Technology Facilities Council through grant numbers ST/P004598/1 and ST/V001027/1. B.S.N.S would like to acknowledge the financial support of the UKRI STFC through Grants No. ST/T001739/1 and ST/P005101/1. T.M., V.A., D.C-O., E.M., A.P., J.P. and D.V. acknowledge funding through the I+D+i, Spain grants FPA2016-76765-P and PGC2018-096717-B-C21 funded by MCIN/AEI/10.13039/501100011033; and by the European Commission H2020 Framework Programme project ENSAR2 (Grant agreement ID: 654002). Partially funded by Spanish MCIN/AEI and European RDF grants PID2019-104714GB-C2 and FPA2017-83946-C2, and Generalitat Valenciana, Spain PROMETEO/2019/007.

References

[1] M. Pfützner, P. Armbruster, T. Baumann, J. Benlliure, M. Bernas, W.N. Catford, D. Cortina-Gil, J.M. Daugas, H. Geissel, M. Górska, H. Grawe, R. Grzywacz, M. Hellström, N. Iwasa, Z. Janas, A. Junghans, M. Karny, S. Leenhardt, M. Lewitowicz, A.C. Mueller, F. de Oliviera, P.H. Regan, M. Rejmund, K. Rykaczewski, K. Sümmerer, New isotopes and isomers produced by the fragmentation of ^{238}UU at 1000 MeV/nucleon, Phys. Lett. B 444 (1) (1998) 32–37, http://dx.doi.org/10.1016/S0370-2693(98)01332-X, URL https://www.sciencedirect.com/science/article/pii/S037026939801332X.

[2] C. Hinke, M. Böhmer, P. Boutachkov, T. Faestermann, H. Geissel, J. Gerl, R. Gernhäuser, M. Górska, A. Gottardo, H. Grawe, J.L. Grebosz, R. Krücken, N. Kurz, Z. Liu, L. Maier, F. Nowacki, S. Pietri, Z. Podolyák, K. Sieja, K. Steiger, K. Straub, H. Weick, H.-J. Wollersheim, P.J. Woods, N. Al-Dahan, N. Alkhomashi, A. Ataç, A. Blazhev, N.F. Braun, I.T. Čeliković, T. Davinson, I. Dillmann, C. Domingo-Pardo, P.C. Doornenbal, G. de France, G.F. Farrelly, F. Farinon, N. Goel, T.C. Habermann, R. Hoischen, R. Janik, M. Karny, A. Kaşkaş, I.M. Kojouharov, T. Kröll, Y. Litvinov, S. Myalski, F. Nebel, S. Nishimura, C. Nociforo, J. Nyberg, A.R. Parikh, A. Procházka, P.H. Regan, C. Rigollet, H. Schaffner, C. Scheidenberger, S. Schwertel, P.-A. Söderström, S.J. Steer, A. Stolz, P. Strmeň, Superallowed Gamow–Teller decay of the doubly magic nucleus ^{100}Sn, Nature 486 (2012) 341–345, http://dx.doi.org/10.1038/nature11116, URL https://www.nature.com/articles/nature11116.

[3] H. Geissel, P. Armbruster, K.H. Behr, A. Brünle, K. Burkard, M. Chen, H. Folger, B. Franczak, H. Keller, O. Klepper, B. Langenbeck, F. Nickel, E. Pfeng, M. Pfützner, E. Roeckl, K. Rykaczewski, I. Schall, D. Schardt, C. Scheidenberger, K.-H. Schmidt, A. Schröter, T. Schwab, K. Sümmerer, M. Weber, G. Münzenberg, T. Brohm, H.-G. Clerc, M. Fauerbach, J.-J. Gaimard, A. Grewe, E. Hanelt, B. Knödler, M. Steiner, B. Voss, J. Weckenmann, C. Ziegler, A. Magel, H. Wollnik, J.P. Dufour, Y. Fujita, D.J. Vieira, B. Sherrill, The GSI projectile fragment separator (FRS): a versatile magnetic system for relativistic heavy ions, Nucl. Instrum. Methods Phys. Res. B 70 (1) (1992) 286–297, http://dx.doi.org/10.1016/0168-583X(92)95944-M, URL https://www.sciencedirect.com/science/article/pii/0168583X9295944M.

[4] H. Geissel, H. Weick, M. Winkler, G. Münzenberg, V. Chichkine, M. Yavor, T. Aumann, K.H. Behr, M. Böhmer, A. Brünle, K. Burkard, J. Benlliure, D. Cortina-Gil, L. Chulkov, A. Dael, J.-E. Ducret, H. Emling, B. Franczak, J. Friese, B. Gastineau, J. Gerl, R. Gernhäuser, M. Hellström, B. Jonson, J. Kojouharova, R. Kulessa, B. Kindler, N. Kurz, B. Lommel, W. Mittig, G. Moritz, C. Mühle, J. Nolen, G. Nyman, P. Roussel-Chomaz, C. Scheidenberger, K.-H. Schmidt, G. Schrieder, B.M. Sherrill, H. Simon, K. Sümmerer, N.A. Tahir, V. Vysotsky, H. Wollnik, A.F. Zeller, The super-FRS project at GSI, Nucl. Instrum. Methods Phys. Res. B 204 (2003) 71–85, http://dx.doi.org/10.1016/S0168-583X(02)01893-1, URL https://www.sciencedirect.com/science/article/pii/S0168583X02018931, 14th International Conference on Electromagnetic Isotope Separators and Techniques Related to their Applications.

[5] P. Spiller, G. Franchetti, The FAIR accelerator project at GSI, Nucl. Instrum. Methods Phys. Res. A 561 (2) (2006) 305–309, http://dx.doi.org/10.1016/j.nima.2006.01.043, URL https://www.sciencedirect.com/science/article/pii/S0168900206000507, Proceedings of the Workshop on High Intensity Beam Dynamics.

[6] B. Rubio, Decay spectroscopy (DESPEC) at the new FAIR-NUSTAR facility, Internat. J. Modern Phys. E 15 (08) (2006) 1979–1988, http://dx.doi.org/10.1142/S0218301306005484.

[7] J. Gerl, Nuclear spectroscopy studies at GSI - from RISING to HISPEC/DESPEC, Acta Phys. Pol. B40, 767–778.

[8] Z. Podolyák, From RISING to HISPEC/DESPEC, Nucl. Instrum. Methods Phys. Res. B 266 (19) (2008) 4589–4594, http://dx.doi.org/10.1016/j.nimb.2008.05.106, URL https://www.sciencedirect.com/science/article/pii/S0168583X08007829, Proceedings of the XVth International Conference on Electromagnetic Isotope Separators and Techniques Related to their Applications.

[9] R.B. Cakirli, R.F. Casten, K. Blaum, Correlations of experimental isotope shifts with spectroscopic and mass observables, Phys. Rev. C 82 (2010) 061306, http://dx.doi.org/10.1103/PhysRevC.82.061306, URL https://link.aps.org/doi/10.1103/PhysRevC.82.061306.

[10] https://fair-center.eu/for-users/experiments/nustar/documents/technical-design-reports/nustar-tdr-overview.html. (Accessed 20 October 2021).

[11] AIDA GSI/RIKEN Technical Article, in preparation.

[12] O. Hall, T. Davinson, A. Estrade, J. Liu, G. Lorusso, F. Montes, S. Nishimura, V.H. Phong, P.J. Woods, J. Agramunt, D.S. Ahn, A. Algora, J.M. Allmond, H. Baba, S. Bae, N.T. Brewer, C. Bruno, R. Caballero-Folch, F. Calviño, P.J. Coleman-Smith, G. Cortes, I. Dillmann, C. Domingo-Pardo, A. Fijalkowska, N. Fukuda, S. Go, C.J. Griffin, R. Grzywacz, J. Ha, L.J. Harkness-Brennan, T. Isobe, D. Kahl, L.H. Khiem, G.G. Kiss, A. Korgul, S. Kubono, M. Labiche, I. Lazarus, J. Liang, Z. Liu, K. Matsui, K. Miernik, B. Moon, A.I. Morales, P. Morrall, M.R. Mumpower, N. Nepal, R.D. Page, M. Piersa, V. Pucknell, B.C. Rasco, B. Rubio, K. Rykaczewski, H. Sakurai, Y. Shimizu, D. Stracener, T. Sumikama, H. Suzuki, J. Tain, H. Takeda, A. Tarifeño-Saldivia, A. Tolosa-Delgado, M. Wolińska-Cichocka, R. Yokoyama, β-Delayed neutron emission of r-process nuclei at the N=82 shell closure, Phys. Lett. B 816 (2021) 136266, http://dx.doi.org/10.1016/j.physletb.2021.136266, URL https://www.sciencedirect.com/science/article/pii/S0370269321002069.

[13] G.S. Li, C. Lizarazo, J. Gerl, I. Kojouharov, H. Schaffner, M. Górska, N. Pietralla, S. Saha, M.L. Liu, J.G. Wang, Simulated characteristics of the DEGAS γ-detector array, Nucl. Instrum. Methods Phys. Res. A 890 (2018) 148–154, http://dx.doi.org/10.1016/j.nima.2018.02.062, URL https://www.sciencedirect.com/science/article/pii/S016890021830216X.

[14] M. Doncel, B. Cederwall, S. Martín, B. Quintana, A. Gadea, E. Farnea, A. Algora, Conceptual design of a high resolution ge array with tracking and imaging capabilities for the DESPEC (FAIR) experiment, J. Instrum. 10 (06) (2015) P06010, http://dx.doi.org/10.1088/1748-0221/10/06/p06010.

[15] M. Rudigier, Z. Podolyák, P.H. Regan, A.M. Bruce, S. Lalkovski, R.L. Canavan, E.R. Gamba, O. Roberts, I. Burrows, D.M. Cullen, L.M. Fraile, L. Gerhard, J. Gerl, M. Gorska, A. Grant, J. Jolie, V. Karayonchev, N. Kurz, W. Korten, I.H. Lazarus, C.R. Nita, V.F.E. Pucknell, J.-M. Régis, H. Schaffner, J. Simpson, P. Singh, C.M. Townsley, J. Smith, J. Vesic, FATIMA — FAst TIMing Array for DESPEC at FAIR, Nucl. Instrum. Methods Phys. Res. A 969 (2020) 163967, http://dx.doi.org/10.1016/j.nima.2020.163967, URL http://www.sciencedirect.com/science/article/pii/S0168900220304332.

[16] A. Torner, J. Agramunt, A. Algora, L. Batet, R. Caballero-Folch, F. Calviño, D. Cano-Ott, A. García, G. Cortés, I. Dillmann, C. Domingo-Pardo, M. Gómez-Hornillos, V. Gorlychev, M. Marta, T. Martínez, A. Poch, C. Pretel, A. Riego, J. Taín, TEchnical Design Report of the Beta-Delayed Neutron Detector (BELEN) for NUSTAR (DESPEC), Technical Report, Universitat PolitÈcnica de Catalunya, Barcelona, Spain, 2014, URL https://fair-center.eu/fileadmin/fair/publications_exp/TDR_HISPEC_DESPEC_BELEN_public.pdf.

[17] T. Martínez, D. Cano-Ott, J. Castilla, A.R. García, J. Marin, G. Martinez, E. Mendoza, C. Santos, F.J. Tera, D. Villamarin, J. Agramunt, A. Algora, C. Domingo, M.D. Jordan, B. Rubio, J. Taín, C. Bhattacharya, K. Banerjee, S. Bhattacharya, P. Roy, J.K. Meena, S. Kundu, G. Mukherjee, T.K. Ghosh, T.K. Rana, R. Pandey, A. Saxena, B. Behera, H. Penttilä, A. Jokinen, S. Rinta-Antila, C. Guerrero, M.C. Ovejero, MONSTER: a TOF spectrometer for β-delayed neutron spectroscopy, Nucl. Data Sheets 120 (2014) 78–80, http://dx.doi.org/10.1016/j.nds.2014.07.011, URL https://www.sciencedirect.com/science/article/pii/S0090375214004633.

[18] J.L. Tain, A. Algora, J. Agramunt, V. Guadilla, M.D. Jordan, A. Montaner-Pizá, B. Rubio, E. Valencia, D. Cano-Ott, W. Gelletly, T. Martinez, E. Mendoza, Z. Podolyák, P. Regan, J. Simpson, A.J. Smith, J. Strachan, A decay total absorption spectrometer for DESPEC at FAIR, Nucl. Instrum. Methods Phys. Res. A 803 (2015) 36–46, http://dx.doi.org/10.1016/j.nima.2015.09.009, URL https://www.sciencedirect.com/science/article/pii/S016890021501058X.

[19] V. Guadilla, J.L. Tain, A. Algora, J. Agramunt, J. Äystö, J.A. Briz, A. Cucoanes, T. Eronen, M. Estienne, M. Fallot, L.M. Fraile, E. Ganioğlu, W. Gelletly, D. Gorelov, J. Hakala, A. Jokinen, D. Jordan, A. Kankainen, V. Kolhinen, J. Koponen, M. Lebois, L. Le Meur, T. Martinez, M. Monserrate, A. Montaner-Pizá, I. Moore, E. Nácher, S.E.A. Orrigo, H. Penttilä, I. Pohjalainen, A. Porta, J. Reinikainen, M. Reponen, S. Rice, S. Rinta-Antila, B. Rubio, K. Rytkönen, T. Shiba, V. Sonnenschein, A.A. Sonzogni, E. Valencia, V. Vedia, A. Voss, J. Wilson, A.-A. Zakari-Issoufou, Characterization and performance of the DTAS detector, Nucl. Instrum. Methods Phys. Res. A 910 (2018) 79–89, http://dx.doi.org/10.1016/j.nima.2018.09.001, URL https://www.sciencedirect.com/science/article/pii/S0168900218310799.

[20] M. Polettini, S. Jazrawi, M. Chishti, A. Yaneva, B. Das, A. Banerjee, N. Hubbard, A. Mistry, H. Albers, R. Shearman, DESPEC phase-0 campaign at GSI, in: SIFCongress, Sep 2020, Milano, 2020, p. 67, http://dx.doi.org/10.1393/ncc/i2021-21067-8, URL https://hal.archives-ouvertes.fr/hal-03323220/.

[21] H. Geissel, G. Münzenberg, C. Scheidenberger, 25 Years of FRS experiments and new horizons, in: S. Schramm, M. Schäfer (Eds.), New Horizons in Fundamental Physics, Springer International Publishing, Cham, 2017, pp. 55–79, http://dx.doi.org/10.1007/978-3-319-44165-8_5.

[22] J. Simpson, The Euroball spectrometer, Z. Phys. A 358 (1997) 139–143.

[23] A. Tolosa-Delgado, J. Agramunt, J.L. Tain, A. Algora, C. Domingo-Pardo, A.I. Morales, B. Rubio, A. Tarifeño-Saldivia, F. Calviño, G. Cortes, N.T. Brewer, B.C. Rasco, K.P. Rykaczewski, D.W. Stracener, J.M. Allmond, R. Grzywacz, R. Yokoyama, M. Singh, T. King, M. Madurga, S. Nishimura, V.H. Phong, S. Go, J. Liu, K. Matsui, H. Sakurai, G.G. Kiss, T. Isobe, H. Baba, S. Kubono, N. Fukuda, D. Ahn, Y. Shimizu, T. Sumikama, H. Suzuki, H. Takeda, P.A. Söderström, M. Takechi, C. Bruno, T. Davinson, C.J. Griffin, O. Hall, D. Kahl, P.J. Woods, P.J. Coleman-Smith, M. Labiche, I. Lazarus, P. Morrall, V.E. Pucknell, J. Simpson, S.L. Thomas, M. Prydderch, L.J. Harkness-Brennan, R.D. Page, I. Dillmann, R. Caballero-Folch, Y. Saito, A. Estrade, N. Nepal, F. Montes, G. Lorusso, J. Liang, S. Bae, J. Ha, B. Moon, Commissioning of the BRIKEN detector for the measurement of very exotic β-delayed neutron emitters, Nucl. Instrum. Methods Phys. Res. A 925 (2019) 133–147, http://dx.doi.org/10.1016/j.nima.2019.02.004, URL https://www.sciencedirect.com/science/article/pii/S0168900219301743.

[24] D. Braga, P.J. Coleman-Smith, T. Davinson, I.H. Lazarus, R.D. Page, S. Thomas, AIDA: A 16-channel amplifier ASIC to read out the advanced implantation detector array for experiments in nuclear decay spectroscopy, in: 2011 2nd International Conference on Advancements in Nuclear Instrumentation, Measurement Methods and their Applications, 2011, pp. 1–5.

[25] I. Lazarus, E. Appelbe, P. Butler, P. Coleman-Smith, J. Cresswell, S. Freeman, R. Herzberg, I. Hibbert, D. Joss, S. Letts, R. Page, V. Pucknell, P. Regan, J. Sampson, J. Simpson, J. Thornhill, R. Wadsworth, The GREAT triggerless total data readout method, IEEE Trans. Nucl. Sci. 48 (3) (2001) 567–569, http://dx.doi.org/10.1109/23.940120.

[26] J. Serrano, P. Alvarez, M. Cattin, E.G. Cota, P.M. J. H. Lewis, T. Włostowski, G. Daniluk, M. Lipinski, The white rabbit project, in: Proceedings of ICALEPCS TUC004, Kobe, Japan, 2009.

[27] GREAT with MIDAS, 2021, http://npg.dl.ac.uk/documents/edoc504/edoc504.html. (Accessed 20 October 2021).

[28] V. Pucknell, The MIDAS multi instance data acquisition system, 2021, http://npg.dl.ac.uk/MIDAS. (Accessed 20 October 2021).

[29] Saint-gobain website: Crystals, 2021, http://www.crystals.saint-gobain.com/. (Accessed 20 October 2021).

[30] Sensl: C-series datasheet, 2021, http://sensl.com/downloads/ds/DS-MicroCseries.pdf. (Accessed 20 October 2021).

[31] A. Banerjee, M. Wiebusch, M. Polettini, A. Mistry, H. Heggen, H. Schaffner, H.M. Albers, N. Kurz, M. Górska, J. Gerl, Analog front-end for FPGA-based readout electronics for scintillation detectors, Nucl. Instrum. Methods Phys. Res. A 1028 (2022) 166357, http://dx.doi.org/10.1016/j.nima.2022.166357, URL https://www.sciencedirect.com/science/article/pii/S0168900222000389.

[32] H. Mach, R. Gill, M. Moszyński, A method for picosecond lifetime measurements for neutron-rich nuclei: (1) outline of the method, Nucl. Instrum. Methods Phys. Res. A 280 (1) (1989) 49–72, http://dx.doi.org/10.1016/0168-9002(89)91272-2, URL https://www.sciencedirect.com/science/article/pii/0168900289912722.

[33] J.-M. Régis, G. Pascovici, J. Jolie, M. Rudigier, The mirror symmetric centroid difference method for picosecond lifetime measurements via γ-γ coincidences using very fast LaBr3(Ce) scintillator detectors, Nucl. Instrum. Methods Phys. Res. A 622 (1) (2010) 83–92, http://dx.doi.org/10.1016/j.nima.2010.07.047, URL https://www.sciencedirect.com/science/article/pii/S0168900210016578.

[34] A. Goasduff, D. Mengoni, F. Recchia, J.J. Valiente-Dobon, R. Menegazzo, G. Benzoni, D. Barrientos, M. Bellato, N. Bez, M. Biasotto, N. Blasi, C. Boiano, A. Boso, S. Bottoni, A. Bracco, S. Brambilla, D. Brugnara, F. Camera, S. Capra, A. Capsoni, P. Cocconi, S. Coelli, M.L. Cortes, F.C.L. Crespi, G. de Angelis, F.J. Egea, C. Fanin, S. Fantinel, A. Gadea, E.R. Gamba, A. Gambalonga, C. Gesmundo, G. Gosta, A. Gottardo, A. Gozzelino, E.T. Gregor, M. Gulmini, J. Ha, K. Hadyaska-Klek, A. Illana, R. Isocrate, G. Jaworski, P.R. John, S.M. Lenzi, S. Leoni, S. Lunardi, M. Magalini, N. Marchini, B. Million, V. Modamio, A. Nannini, D.R. Napoli, G. Pasqualato, J. Pellumaj, R.M. Perez-Vidal, S. Pigliapoco, M. Polettini, C. Porzio, A. Pullia, L. Ramina, G. Rampazzo, M. Rampazzo, M. Rebeschini, K. Rezynkina, M. Rocchini, M. Romanato, D. Rosso, A. Saltarelli, M. Scarcioffolo, M. Siciliano, D.A. Testov, D. Tomasella, F. Tomasi, N. Toniolo, C.A. Ur, S. Ventura, F. Veronese, E. Viscione, V. Volpe, O. Wieland, I. Zanon, S. Ziliani, G. Zhang, D. Bazzacco, The GALILEO Gamma-ray array at the legnaro national laboratories, Nucl. Instrum. Methods Phys. Res. A 1015 (2021) 165753, http://dx.doi.org/10.1016/j.nima.2021.165753, URL https://www.sciencedirect.com/science/article/pii/S0168900221007385.

[35] P.R. John, H.G. Thomas, R. Menegazzo, J.J. Valiente-Dobon, I. Kojouharov, V. Werner, N. Pietralla, A. Pullia, D. Bazzacco, G. Benzoni, G. Pasqualato, D. Mengoni, D.R. Napoli, F. Recchia, Assembly of 8 Galileo TC at Institut für Kernphysik TU Darmstadt for the DESPEC Campaign, LNL Annual Report 2020, 2019, URL https://www1.lnl.infn.it/~annrep/read_ar/2019/contributions/pdfs/032_A_71_A66.pdf.

[36] J. Hoffmann, New TASCA data acquisition hardware development for the search of element 119 and 120, GSI Sci. Rep. 2011 253 (13) (2012).

[37] H.J. Wollersheim, D.E. Appelbe, A. Banu, R. Bassini, T. Beck, F. Becker, P. Bednarczyk, K.-H. Behr, M.A. Bentley, G. Benzoni, C. Boiano, U. Bonnes, A. Bracco, S. Brambilla, A. Brünle, A. Bürger, K. Burkard, P. Butler, F. Camera, D. Curien, J. Devin, P. Doornenbal, C. Fahlander, K. Fayz, H. Geissel, J. Gerl, M. Górska, H. Grawe, J. Grębosz, R. Griffiths, G. Hammond, M. Hellström, J. Hoffmann, H. Hübel, J. Jolie, J. Kalben, M. Kmiecik, I. Kojouharov, R. Kulessa, N. Kurz, I. Lazarus, J. Li, J. Leske, R. Lozeva, A. Maj, S. Mandal, W. Męczyński, B. Million, G. Münzenberg, S. Muralithar, M. Mutterer, P. Nolan, G. Neyens, J. Nyberg, W. Prokopowicz, V.F.E. Pucknell, P. Reiter, D. Rudolph, N. Saito, T.R. Saito, D. Seddon, H. Schaffner, J. Simpson, K.-H. Speidel, J. Styczeń, K. Sümmerer, N. Warr, H. Weick, C. Wheldon, O. Wieland, M. Winkler, M. Zięblíński, Rare ISotopes INvestigation at GSI (RISING) using gamma-ray spectroscopy at relativistic energies, Nucl. Instrum. Methods Phys. Res. A 537 (3) (2005) 637–657, http://dx.doi.org/10.1016/j.nima.2004.08.072, URL https://www.sciencedirect.com/science/article/pii/S0168900204019588.

[38] https://epics-controls.org/. (Accessed 07 February 2022).

[39] G.S. Li, R. Lozeva, I. Kojouharov, J. Gerl, M. Górska, Characteristics of the DEGAS-FATIMA hybrid setup for the DESPEC program at NUSTAR, Nucl. Instrum. Methods Phys. Res. A 987 (2021) 164806, http://dx.doi.org/10.1016/j.nima.2020.164806, URL https://www.sciencedirect.com/science/article/pii/S0168900220312031.

[40] M. Karny, J.M. Nitschke, L.F. Archambault, K. Burkard, D. Cano-Ott, M. Hellström, W. Hüller, R. Kirchner, S. Lewandowski, E. Roeckl, A. Sulik, Coupling a total absorption spectrometer to the GSI on-line mass separator, Nucl. Instrum. Methods Phys. Res. A 126 (1) (1997) 411–415, http://dx.doi.org/10.1016/S0168-583X(96)01007-5, URL https://www.sciencedirect.com/science/article/pii/S0168583X96010075, International Conference on Electromagnetic Isotope Separators and Techniques Related to Their Applications.

[41] V. Guadilla, J.L. Tain, A. Algora, J. Agramunt, D. Jordan, M. Monserrate, A. Montaner-Pizá, E. Nácher, S.E.A. Orrigo, B. Rubio, E. Valencia, M. Estienne, M. Fallot, L. Le Meur, J.A. Briz, A. Cucoanes, A. Porta, T. Shiba, A.-A. Zakari-Issoufou, A.A. Sonzogni, J. Äystö, T. Eronen, D. Gorelov, J. Hakala, A. Jokinen, A. Kankainen, V.S. Kolhinen, J. Koponen, I.D. Moore, H. Penttilä, I. Pohjalainen, J. Reinikainen, M. Reponen, S. Rinta-Antila, K. Rytkönen, V. Sonnenschein, A. Voss, L.M. Fraile, V. Vedia, E. Ganioğlu, W. Gelletly, M. Lebois, J.N. Wilson, T. Martinez, Total absorption γ-ray spectroscopy of the β-delayed neutron emitters ^{137}I and ^{95}Rb, Phys. Rev. C 100 (2019) 044305, http://dx.doi.org/10.1103/PhysRevC.100.044305, URL https://link.aps.org/doi/10.1103/PhysRevC.100.044305.

[42] V. Guadilla, A. Algora, J. Tain, J. Agramunt, J. Äystö, J. Briz, D. Cano-Ott, A. Cucoanes, T. Eronen, M. Estienne, M. Fallot, L. Fraile, E. Ganioglu, W. Gelletly, D. Gorelov, J. Hakala, A. Jokinen, D. Jordan, A. Kankainen, V. Kolhinen, J. Koponen, M. Lebois, T. Martinez, M. Monserrate, A. Montaner-Pizá, I. Moore, E. Nácher, S. Orrigo, H. Penttilä, Z. Podolyak, I. Pohjalainen, A. Porta, P. Regan, J. Reinikainen, M. Reponen, S. Rinta-Antila, B. Rubio, K. Rytkönen, T. Shiba, V. Sonnenschein, A. Sonzogni, E. Valencia, V. Vedia, A.

Voss, J. Wilson, A.-A. Zakari-Issoufou, First experiment with the NUSTAR/FAIR decay total absorption γ-ray spectrometer (DTAS) at the IGISOL IV facility, Nucl. Instrum. Methods Phys. Res. B 376 (2016) 334–337, http://dx.doi.org/10.1016/j.nimb.2015.12.018, URL https://www.sciencedirect.com/science/article/pii/S0168583X15012628, Proceedings of the XVIIth International Conference on Electromagnetic Isotope Separators and Related Topics (EMIS2015), Grand Rapids, MI, U.S.A., 11-15 May 2015.

[43] V. Guadilla, A. Algora, J.L. Tain, J. Agramunt, D. Jordan, A. Montaner-Pizá, S.E.A. Orrigo, B. Rubio, E. Valencia, J. Suhonen, O. Civitarese, J. Äystö, J.A. Briz, A. Cucoanes, T. Eronen, M. Estienne, M. Fallot, L.M. Fraile, E. Ganioğlu, W. Gelletly, D. Gorelov, J. Hakala, A. Jokinen, A. Kankainen, V. Kolhinen, J. Koponen, M. Lebois, T. Martinez, M. Monserrate, I. Moore, E. Nácher, H. Penttilä, I. Pohjalainen, A. Porta, J. Reinikainen, M. Reponen, S. Rinta-Antila, K. Rytkönen, T. Shiba, V. Sonnenschein, A.A. Sonzogni, V. Vedia, A. Voss, J.N. Wilson, A.-A. Zakari-Issoufou, Experimental study of ^{100}Tc β decay with total absorption γ-ray spectroscopy, Phys. Rev. C 96 (2017) 014319, http://dx.doi.org/10.1103/PhysRevC.96.014319, URL https://link.aps.org/doi/10.1103/PhysRevC.96.014319.

[44] V. Guadilla, A. Algora, J.L. Tain, M. Estienne, M. Fallot, A.A. Sonzogni, J. Agramunt, J. Äystö, J.A. Briz, A. Cucoanes, T. Eronen, L.M. Fraile, E. Ganioğlu, W. Gelletly, D. Gorelov, J. Hakala, A. Jokinen, D. Jordan, A. Kankainen, V. Kolhinen, J. Koponen, M. Lebois, L. Le Meur, T. Martinez, M. Monserrate, A. Montaner-Pizá, I. Moore, E. Nácher, S.E.A. Orrigo, H. Penttilä, I. Pohjalainen, A. Porta, J. Reinikainen, M. Reponen, S. Rinta-Antila, B. Rubio, K. Rytkönen, T. Shiba, V. Sonnenschein, E. Valencia, V. Vedia, A. Voss, J.N. Wilson, A.-A. Zakari-Issoufou, Large impact of the decay of niobium isomers on the reactor $\bar{\nu}_e$ summation calculations, Phys. Rev. Lett. 122 (2019) 042502, http://dx.doi.org/10.1103/PhysRevLett.122.042502, URL https://link.aps.org/doi/10.1103/PhysRevLett.122.042502.

[45] V. Guadilla, A. Algora, J.L. Tain, J. Agramunt, J. Äystö, J.A. Briz, A. Cucoanes, T. Eronen, M. Estienne, M. Fallot, L.M. Fraile, E. Ganioğlu, W. Gelletly, D. Gorelov, J. Hakala, A. Jokinen, D. Jordan, A. Kankainen, V. Kolhinen, J. Koponen, M. Lebois, L. Le Meur, T. Martinez, M. Monserrate, A. Montaner-Pizá, I. Moore, E. Nácher, S.E.A. Orrigo, H. Penttilä, I. Pohjalainen, A. Porta, J. Reinikainen, M. Reponen, S. Rinta-Antila, B. Rubio, K. Rytkönen, P. Sarriguren, T. Shiba, V. Sonnenschein, A.A. Sonzogni, E. Valencia, V. Vedia, A. Voss, J.N. Wilson, A.-A. Zakari-Issoufou, Total absorption γ-ray spectroscopy of niobium isomers, Phys. Rev. C 100 (2019) 024311, http://dx.doi.org/10.1103/PhysRevC.100.024311, URL https://link.aps.org/doi/10.1103/PhysRevC.100.024311.

[46] V. Guadilla, J.L. Tain, A. Algora, J. Agramunt, D. Jordan, M. Monserrate, A. Montaner-Pizá, S.E.A. Orrigo, B. Rubio, E. Valencia, J.A. Briz, A. Cucoanes, M. Estienne, M. Fallot, L. Le Meur, A. Porta, T. Shiba, A.-A. Zakari-Issoufou, J. Äystö, T. Eronen, D. Gorelov, J. Hakala, A. Jokinen, A. Kankainen, V.S. Kolhinen, J. Koponen, I.D. Moore, H. Penttilä, I. Pohjalainen, J. Reinikainen, M. Reponen, S. Rinta-Antila, K. Rytkönen, V. Sonnenschein, A. Voss, L.M. Fraile, V. Vedia, E. Ganioğlu, W. Gelletly, M. Lebois, J.N. Wilson, T. Martinez, E. Nácher, A.A. Sonzogni, Determination of β-decay ground state feeding of nuclei of importance for reactor applications, Phys. Rev. C 102 (2020) 064304, http://dx.doi.org/10.1103/PhysRevC.102.064304, URL https://link.aps.org/doi/10.1103/PhysRevC.102.064304.

[47] A. Algora, J. Tain, B. Rubio, M. Fallot, W. Gellety, Beta-decay studies for applied and basic nuclear physics, Eur. Phys. J. A 57 (2021) 85, http://dx.doi.org/10.1140/epja/s10050-020-00316-4.

[48] A. Algora, J.A. Victoria, B. Rubio, J.L. Tain, A. Tolosa, J. Agramunt, E. Nacher, S.E.A. Orrigo, V. Guadilla, G. Kiss, D. Sohler, I. Kuti, T. Davinson, O.B. Hall, D.M. Kahl, C.G. Bruno, C.J. Appleton, P.J. Woods, S. Nishimura, N. Fukuda, H. Suzuki, D.S. Ahn, H. Baba, Y. Shimizu, H. Takeda, D. Nishimura, T. Isobe, M. Kaneko, S. Kubono, H. Sakurai, H. Shimizu, T. Sumikama, P. Doornenbal, M.L. Cortes, Z. Podolyak, W. Gelletly, E. Ganioglu, Y. Fujita, F. Molina, J. Liu, J. Lee, K.P. Rykaczewski, M. Wolinska-Cichocka, M. Labiche, C.J. Griffin, S. Bae, J. Ha, Y. Litvinov, Total absorption gamma spectroscopy studies around ^{100}Sn, in: RIKEN Accelerator Progress Report, Vol. 53, 2019, p. 30.

[49] R. Caballero-Folch, C. Domingo-Pardo, J. Agramunt, A. Algora, F. Ameil, A. Arcones, Y. Ayyad, J. Benlliure, I.N. Borzov, M. Bowry, F. Calviño, D. Cano-Ott, G. Cortés, T. Davinson, I. Dillmann, A. Estrade, A. Evdokimov, T. Faestermann, F. Farinon, D. Galaviz, A.R. García, H. Geissel, W. Gelletly, R. Gernhäuser, M.B. Gómez-Hornillos, C. Guerrero, M. Heil, C. Hinke, R. Knöbel, I. Kojouharov, J. Kurcewicz, N. Kurz, Y.A. Litvinov, L. Maier, J. Marganiec, T. Marketin, M. Marta, T. Martínez, G. Martínez-Pinedo, F. Montes, I. Mukha, D.R. Napoli, C. Nociforo, C. Paradela, S. Pietri, Z. Podolyák, A. Prochazka, S. Rice, A. Riego, B. Rubio, H. Schaffner, C. Scheidenberger, K. Smith, E. Sokol, K. Steiger, B. Sun, J.L. Taín, M. Takechi, D. Testov, H. Weick, E. Wilson, J.S. Winfield, R. Wood, P. Woods, A. Yeremin, First measurement of several β-delayed neutron emitting isotopes beyond N= 126, Phys. Rev. Lett. 117 (2016) 012501, http://dx.doi.org/10.1103/PhysRevLett.117.012501, URL https://link.aps.org/doi/10.1103/PhysRevLett.117.012501.

[50] J. Agramunt, A. García, A. Algora, J. Äystö, R. Caballero-Folch, F. Calviño, D. Cano-Ott, G. Cortés, C. Domingo-Pardo, T. Eronen, W. Gelletly, M. Gómez-Hornillos, J. Hakala, A. Jokinen, D. Jordan, A. Kankainen, V. Kolkinen, T. Martínez, P. Mason, I. Moore, H. Penttilä, Z. Podolyák, M. Reponen, A. Riego, J. Rissanen, B. Rubio, A. Saastamoinen, J. Tain, E. Valencia, New beta-delayed neutron measurements in the light-mass fission group, Nucl. Data Sheets 120 (2014) 74–77, http://dx.doi.org/10.1016/j.nds.2014.07.010, URL https://www.sciencedirect.com/science/article/pii/S0090375214004621.

[51] A.R. Garcia, T. Martínez, D. Cano-Ott, J. Castilla, C. Guerrero, J. Marín, G. Martínez, E. Mendoza, M.C. Ovejero, E.M. Reillo, C. Santos, F.J. Tera, D. Villamarín, R. Nolte, J. Agramunt, A. Algora, J.L. Tain, K. Banerjee, C. Bhattacharya, H. Pentillä, S. Rinta-Antila, D. Gorelov, MONSTER: a time of flight spectrometer for β-delayed neutron emission measurements, J. Instrum. 7 (05) (2012) C05012, http://dx.doi.org/10.1088/1748-0221/7/05/c05012, URL https://iopscience.iop.org/article/10.1088/1748-0221/7/05/C05012.

[52] https://fair-center.eu/for-users/experiments/nustar/documents/technical-design-reports.html. (Accessed 20 October 2021).

[53] J. Adamczewski-Musch, B. Bellenot, A. Linev, Web interface for online ROOT and DAQ applications, in: 2014 19th IEEE-NPSS Real Time Conference, 2014, pp. 1–5, http://dx.doi.org/10.1109/RTC.2014.7097456.

[54] J. Adamczewski-Musch, T. Stibor, Mass storage interface LTSM for FAIR phase 0 data acquisition, EPJ Web Conf. 245 (2020) 01018, http://dx.doi.org/10.1051/epjconf/202024501018.

[55] GSI multi branch system (MBS), 2021, https://www.gsi.de/en/work/research/experiment_electronics/data_processing/data_acquisition/mbs.html. (Accessed 20 October 2021).

[56] General machine timing system at GSI and FAIR, 2021, https://www-acc.gsi.de/wiki/Timing/WebHome. (Accessed 20 October 2021).

[57] PEXARIA5 technical document, 2022, https://www.gsi.de/work/forschung/experimentelektronik/digitalelektronik/digitalelektronik/module/pci_pci_e/pexaria/pexaria5. (Accessed 07 February 2022).

[58] VETAR2 technical document, 2022, https://www.gsi.de/work/forschung/experimentelektronik/digitalelektronik/digitalelektronik/module/vme/vetar/vetar2. (Accessed 07 February 2022).

[59] D. Villamarin, et al., High-performance multi-detector scalable DAQ for nuclear data measurements, in preparation.

[60] J. Agramunt, J.L. Tain, M.B. Gómez-Hornillos, A.R. Garcia, F. Albiol, A. Algora, R. Caballero-Folch, F. Calviño, D. Cano-Ott, G. Cortés, C. Domingo-Pardo, T. Eronen, W. Gelletly, D. Gorelov, V. Gorlychev, H. Hakala, A. Jokinen, M. Jordan, A. Kankainen, V. Kolhinen, L. Kucuk, T. Martinez, P.J.R. Mason, I. Moore, H. Penttilä, Z. Podolyák, C. Pretel, M. Reponen, A. Riego, J. Rissanen, B. Rubio, A. Saastamoinen, A. Tarifeño-Saldivia, E. Valencia, Characterization of a neutron–beta counting system with beta-delayed neutron emitters, Nucl. Instrum. Methods Phys. Res. A 807 (2016) 69–78, http://dx.doi.org/10.1016/j.nima.2015.10.082, URL https://www.sciencedirect.com/science/article/pii/S0168900215013169.

[61] Evaluated nuclear structure data file, 2021, https://www.nndc.bnl.gov/ensdf/. (Accessed 20 October 2021).

[62] Ucesb - unpack and check every single bit, 2021, http://fy.chalmers.se/~f96hajo/ucesb/. (Accessed 20 October 2021).

[63] R. Brun, F. Rademakers, ROOT — An object oriented data analysis framework, Nucl. Instrum. Methods Phys. Res. A 389 (1) (1997) 81–86, http://dx.doi.org/10.1016/S0168-9002(97)00048-X, URL https://www.sciencedirect.com/science/article/pii/S016890029700048X, New Computing Techniques in Physics Research V.

[64] The Go4 Project page, https://www.gsi.de/en/work/research/experiment_electronics/data_processing/data_analysis/the_go4_home_page. (Accessed 20 October 2021).

[65] J. Adamczewski-Musch, N. Kurz, S. Linev, Developments and applications of DAQ framework DABC v2, J. Phys. Conf. Ser. 664 (8) (2015) 082027, http://dx.doi.org/10.1088/1742-6596/664/8/082027.

[66] JSROOT website, 2021, https://root.cern/js/. (Accessed 20 October 2021).

[67] Virgo user manual, 2021, https://hpc.gsi.de/virgo/preface.html. (Accessed 20 October 2021).

[68] A description of the slurm workload manager, 2022, https://slurm.schedmd.com/overview.html. (Accessed 08 February 2022).

[69] M. Al-Turany, D. Bertini, R. Karabowicz, D. Kresan, P. Malzacher, T. Stockmanns, F. Uhlig, The FairRoot framework, J. Phys. Conf. Ser. 396 (2) (2012) 022001, http://dx.doi.org/10.1088/1742-6596/396/2/022001.

[70] S. Myalski, M. Kmiecik, A. Maj, P. Regan, A.B. Garnsworthy, S. Pietri, D. Rudolph, Z. Podolyák, S.J. Steer, F. Becker, P. Bednarczyk, J. Gerl, M. Górska, H. Grawe, I. Kojouharov, H. Schaffner, H.J. Wollersheim, W. Prokopowicz, J. Grebosz, G. Benzoni, Mass and beta decay of ^{34}Si, Acta Phys. Pol. Ser. B 38 (2007).

[71] H. Mach, A. Korgul, M. Górska, H. Grawe, I. Matea, M. Stănoiu, L.M. Fraile, Y.E. Penionzkevich, F.D.O. Santos, D. Verney, S. Lukyanov, B. Cederwall, A. Covello, Z. Dlouhý, B. Fogelberg, G. De France, A. Gargano, G. Georgiev, R. Grzywacz, A.F. Lisetskiy, J. Mrazek, F. Nowacki, W.A. Płóciennik, Z. Podolyák, S. Ray, E. Ruchowska, M.-G. Saint-Laurent, M. Sawicka, C. Stodel, O. Tarasov, Ultrafast-timing lifetime measurements in ^{94}Ru and ^{96}Pd: Breakdown of the seniority scheme in $N = 50$ isotones, Phys. Rev. C 95 (2017) 014313, http://dx.doi.org/10.1103/PhysRevC.95.014313, URL https://link.aps.org/doi/10.1103/PhysRevC.95.014313.

[72] G. Häfner, K. Moschner, A. Blazhev, P. Boutachkov, P.J. Davies, R. Wadsworth, F. Ameil, H. Baba, T. Bäck, M. Dewald, P. Doornenbal, T. Faestermann, A. Gengelbach, J. Gerl, R. Gernhäuser, S. Go, M. Górska, H. Grawe, E. Gregor, H. Hotaka, T. Isobe, D.G. Jenkins, J. Jolie, H.S. Jung, I. Kojouharov, N. Kurz, M. Lewitowicz, G. Lorusso, R. Lozeva, E. Merchan, F. Naqvi, H. Nishibata, D. Nishimura, S. Nishimura, N. Pietralla, H. Schaffner, P.-A. Söderström, K. Steiger, T. Sumikama, J. Taprogge, P. Thöle, H. Watanbe, N. Warr, V. Werner, Z.Y. Xu, A. Yagi, K. Yoshinaga, Y. Zhu, Properties of γ-decaying isomers in the ^{100}Sn region populated in fragmentation of a ^{124}Xe beam, Phys. Rev. C 100 (2019) 024302, http://dx.doi.org/10.1103/PhysRevC.100.024302, URL https://link.aps.org/doi/10.1103/PhysRevC.100.024302.

[73] A.B. Garnsworthy, P.H. Regan, S. Pietri, Y. Sun, F.R. Xu, D. Rudolph, M. Górska, L. Cáceres, Z. Podolyák, S.J. Steer, R. Hoischen, A. Heinz, F. Becker, P. Bednarczyk, P. Doornenbal, H. Geissel, J. Gerl, H. Grawe, J. Grębosz, A. Kelic, I. Kojouharov, N. Kurz, F. Montes, W. Prokopwicz, T. Saito, H. Schaffner, S. Tachenov, E. Werner-Malento, H.J. Wollersheim, G. Benzoni, B. Blank, C. Brandau, A.M. Bruce, F. Camera, W.N. Catford, I.J. Cullen, Z. Dombrádi, E. Estevez, W. Gelletly, G. Ilie, J. Jolie, G.A. Jones, A. Jungclaus, M. Kmiecik, F.G. Kondev, T. Kurtukian-Nieto, S. Lalkovski, Z. Liu, A. Maj, S. Myalski, M. Pfützner, S. Schwertel, T. Shizuma, A.J. Simons, P.M. Walker, O. Wieland, Isomeric states in neutron-deficient *A* 80–90 nuclei populated in the fragmentation of ^{107}Ag, Phys. Rev. C 80 (2009) 064303, http://dx.doi.org/10.1103/PhysRevC.80.064303, URL https://link.aps.org/doi/10.1103/PhysRevC.80.064303.

[74] D. Alber, H. Bertschat, H. Grawe, H. Hass, B. Spellmeyer, Nuclear structure studies of the neutron deficient N=50 nucleus ^{96}Pd, Z. Phys. A 332 (1989) 129–135.

[75] E. Gamba, A Compton-background-correction method for fast-timing measurements using $LaBr_3$ (Ce) detectors: The case of ^{114}Pd (Ph.D. thesis), University of Brighton, 2019.

[76] M.M.R. Chishti, et al., GEANT4 Simulation of FATIMA in preparation.

[77] N. Alkhomashi, P.H. Regan, Z. Podolyák, S. Pietri, A.B. Garnsworthy, S.J. Steer, J. Benlliure, E. Caserejos, R.F. Casten, J. Gerl, H.J. Wollersheim, J. Grebosz, G. Farrelly, M. Górska, I. Kojouharov, H. Schaffner, A. Algora, G. Benzoni, A. Blazhev, P. Boutachkov, A.M. Bruce, A.M.D. Bacelar, I.J. Cullen, L. Cáceres, P. Doornenbal, M.E. Estevez, Y. Fujita, W. Gelletly, R. Hoischen, R. Kumar, N. Kurz, S. Lalkovski, Z. Liu, C. Mihai, F. Molina, A.I. Morales, D. Mücher, W. Prokopowicz, B. Rubio, Y. Shi, A. Tamii, S. Tashenov, J.J. Valiente-Dobón, P.M. Walker, P.J. Woods, F.R. Xu, β^--Delayed spectroscopy of neutron-rich tantalum nuclei: Shape evolution in neutron-rich tungsten isotopes, Phys. Rev. C 80 (2009) 064308, http://dx.doi.org/10.1103/PhysRevC.80.064308, URL https://link.aps.org/doi/10.1103/PhysRevC.80.064308.

[78] C. Lederer, J. Jaklevic, J. Hollander, In-beam gamma-ray spectroscopy of even Mo and Ru isotopes, Nuclear Phys. A 169 (3) (1971) 449–488, http://dx.doi.org/10.1016/0375-9474(71)90697-X, URL https://www.sciencedirect.com/science/article/pii/037594747190697X.

[79] O. Häusser, I. Towner, T. Faestermann, H. Andrews, J. Beene, D. Horn, D. Ward, C. Broude, Magnetic moments of N=50 isotones and proton core polarization, Nuclear Phys. A 293 (1) (1977) 248–268, http://dx.doi.org/10.1016/0375-9474(77)90490-0, URL https://www.sciencedirect.com/science/article/pii/0375947477904900.

[80] E. Nolte, H. Hick, Beta delayed proton emission from the 14s $21/2^+$ spin gap isomer in ^{95}Pd, Z. Phys. A305 (1982) 289.

[81] A.M. Nathan, D.E. Alburger, Mass and beta decay of ^{34}Si, Phys. Rev. C 15 (1977) 1448–1452, http://dx.doi.org/10.1103/PhysRevC.15.1448, URL https://link.aps.org/doi/10.1103/PhysRevC.15.1448.